

Structure-Preserving Geometric Particle-in-Cell Methods for Vlasov-Maxwell Systems

Jianyuan Xiao,¹ Hong Qin,^{1,2,*} and Jian Liu¹

¹*School of Physics, University of Science and Technology of China, Hefei, 230026, China*

²*Plasma Physics Laboratory, Princeton University, Princeton, NJ 08543, U.S.A*

Abstract

Recent development of structure-preserving geometric particle-in-cell (PIC) algorithms for Vlasov-Maxwell systems is summarized. With the arriving of 100 petaflop and exaflop computing power, it is now possible to carry out direct simulations of multi-scale plasma dynamics based on first-principles. However, standard algorithms currently adopted by the plasma physics community do not possess the long-term accuracy and fidelity required in these large-scale simulations. This is because conventional simulation algorithms are based on numerically solving the underpinning differential (or integro-differential) equations, and the algorithms used in general do not preserve the geometric and physical structures of the systems, such as the local energy-momentum conservation law, the symplectic structure, and the gauge symmetry. As a consequence, numerical errors accumulate coherently with time and long-term simulation results are not reliable. To overcome this difficulty and to harness the power of exascale computers, a new generation of structure-preserving geometric PIC algorithms have been developed. This new generation of algorithms utilizes modern mathematical techniques, such as discrete manifolds, interpolating differential forms, and non-canonical symplectic integrators, to ensure gauge symmetry, space-time symmetry and the conservation of charge, energy-momentum, and the symplectic structure. These highly desired properties are difficult to achieve using the conventional PIC algorithms. In addition to summarizing the recent development and demonstrating practical implementations, several new results are also presented, including a structure-preserving geometric relativistic PIC algorithm, the proof of the correspondence between discrete gauge symmetry and discrete charge conservation law, and a reformulation of the explicit non-canonical symplectic algorithm for the discrete Poisson bracket using the variational approach. Numerical examples are given to verify the advantages of the structure-preserving geometric PIC algorithms in comparison with the conventional PIC methods.

* hongqin@ustc.edu.cn

1. INTRODUCTION

Particle-in-Cell (PIC) methods [1–3] have been widely applied since 1960s for simulation studies of plasma physics and beam physics. PIC algorithms numerically solve the Maxwell equations for electromagnetic fields and Newton’s equation for particle dynamics, and therefore can simulate a wide range of collective phenomena in plasmas and charged particle beams. Many PIC algorithms and codes have been developed [4–26]. Why do we need new PIC algorithms? The answer is that standard PIC algorithms do not have the long-term accuracy and fidelity required by the large-scale simulations enabled by the upcoming exascale computing power.

Plasmas and charged particle beams [27] in space and laboratory naturally contain multi-scale structures and dynamics. For example, in a typical tokamak device the operation time is about $10^{10} \sim 10^{14}$ times of electron’s gyro-period. Obviously, it is difficult to carry out first-principle based simulations of these multi-scale structures and dynamics using super computers available today. Recently, computing power over 100 peta floating point operations per second [28, 29] has been built, and exascale computing power is expected to be online in the near future. With these computing power, simulating multi-scale plasma dynamics directly using the PIC method becomes possible. However, standard PIC algorithms currently adopted by the plasma physics community do not possess the long-term accuracy and fidelity that are needed in the study of multi-scale, complex dynamics of plasmas. This is because conventional PIC algorithms are based on numerically solving the underpinning differential (or integro-differential) equations, and the algorithms used in general do not preserve the geometric structures of the physical systems, such as the local energy-momentum conservation law, the symplectic structure, and the gauge symmetry. As a consequence, numerical errors accumulate coherently with time and long-term simulation results are not reliable.

To overcome this serious difficulty and to harness the power of exascale computers, a new generation of structure-preserving geometric PIC algorithms [30–38] have been developed. This new generation of algorithms utilizes modern mathematical techniques, such as discrete manifolds, interpolating differential forms, and non-canonical symplectic integrators, to ensure gauge symmetry, space-time symmetry and the conservation of charge, energy-momentum, and the symplectic structure. These highly desired properties are extremely

difficult to achieve using the conventional PIC algorithms. The purpose of this paper is to summarize the recent development of the structure-preserving geometric PIC methods and to show how to implement such an algorithm for practical purpose. Important theoretical structures and numerical techniques are discussed in details. For example, the correspondence between discrete space-time gauge symmetry and discrete charge conservation law is derived.

Before the technical discussion, we would like to briefly review the historical development of this active research field. Symplectic integrator for finite dimensional ordinary differential equations (ODEs) is the first structure-preserving geometric algorithm systematically studied in 1980s [39–53], even though the idea may have appeared much earlier [54]. In a symplectic method, the discrete one-step iteration map preserves a symplectic 2-form exactly as the exact solution of the Hamiltonian system does. According to theoretical and practical investigations [41, 49, 50, 53], symplectic integrators can globally bound the numerical errors of invariants such as total energy and momentum for all time-steps. For applications to plasma physics and accelerator physics [12, 39, 43], charged particle dynamics, expressed in terms of canonical momentum, admits a canonical symplectic structure and the canonical symplectic integrators apply straightforwardly [39–53]. Recently, explicit high-order non-canonical symplectic methods for single charged particle dynamics in the (\mathbf{x}, \mathbf{v}) coordinates have been discovered [55–59]. For the single guiding-center dynamics in magnetic field, which admits an intrinsically non-canonical symplectic structure [60–62], non-canonical symplectic integrators have been developed [63–69]. If we relax the symplectic constraint to the weaker condition of volume-preserving, a series of volume-preserving algorithms for a single charged particle are available [70–76]. It is interesting to note that the familiar Boris algorithm [77] is volume-preserving but not symplectic [70, 78].

In plasma physics and beam physics, conservative systems often have canonical or non-canonical symplectic structures. But, except for the single charged particle dynamics discussed above, the symplectic structures for most important systems are usually infinite dimensional, such as the Vlasov-Maxwell (VM) systems [79–83], two-fluid model [84], ideal magnetohydrodynamics (MHD) equations [85], and gyrokinetic systems [82, 86–88]. Developing canonical and non-canonical symplectic algorithms for these systems requires techniques to discretize the infinite dimensional symplectic structures. In addition, as physical systems defined on the space-time, these systems also have other important structures inde-

pendent from the symplectic structure, such as the gauge symmetry and charge conservation, the space-time symmetry and energy-momentum conservation. Developing algorithms that are able to preserve these physical structures as well presents new challenges.

The first structure-preserving symplectic PIC algorithm for the VM system was developed by Squire et al. in 2012 [30], and subsequently by Xiao et al. [31, 32]. This is a variational symplectic algorithm based on the geometric discretization in both spatial and temporal dimensions of the action principle for the VM system [86, 87, 89]. The resulting discrete time advance conserves a non-canonical symplectic structure. In 1970s, Lewis proposed to discretize the spatial dimension of the action principle to reduce the system to a set of ODEs without addressing the technique of symplectic time integration [90–93]. We note that symplectic time integration is the most crucial part of the symplectic PIC algorithm for the VM system [30–32]. Of course, Lewis’s idea was before the concept of symplectic integrator was fully developed.

The first non-canonical discrete Poisson bracket for the VM system was given by Xiao et al. in 2015 [33] using a variational method over a discrete space-time manifold with Whitney forms [94] that are appropriately generalized to higher orders. Because the Poisson bracket is non-canonical, it is nontrivial to develop a time advance algorithm that preserves the non-canonical symplectic structure. Fortunately and surprisingly, the explicit high-order splitting time integrator discovered by He et al. [95] for the continuous Morrison-Marsden-Weinstein bracket [79–81] works perfectly for the discrete Poisson bracket. It was adopted by Xiao et al. in Ref. [33] to develop the first explicit high-order non-canonical symplectic PIC algorithm for the VM system. Subsequently, He et al. [35] and Kraus et al. [36] used the method of finite element discrete exterior calculus to discretize the Morrison-Marsden-Weinstein bracket directly. The idea of finite dimensional kinetic system is further studied by Burby [96].

Complementary to the non-canonical symplectic bracket, there also exists a canonical bracket for the VM system, which has been discretized to develop a canonical symplectic PIC algorithm [34].

For the symplectic PIC algorithms of the VM systems described above, the space and time are discretized using different methods. The time advance algorithm in the variational symplectic PIC methods [30–32] is derived from the action discretized in time. Once a temporal discretization is chosen, the time advance algorithm is determined. This type of

time advance is known as the variational symplectic integrator [52]. On the other hand, a splitting method is adopted for the non-canonical symplectic PIC algorithms [33, 35, 36, 97]. In general, splitting methods are applicable to canonical Hamiltonian systems only. In fact, universal symplectic method for general non-canonical systems is not known to exist. However, Crouseilles et al. [98] proposed a splitting method for the non-canonical Poisson bracket of the VM system, which, unfortunately is proven to be incorrect [99]. The correct splitting algorithm is given by He et al. [35] and then quickly applied to the non-canonical symplectic PIC simulations [33, 35, 36, 97].

To preserve the differential form structure of the VM system, it is necessary to select an effective spatial discretization scheme, as first realized by Squire et al. [30], who adopted the method of discrete manifold and Whitney form [94], which was generalized to higher orders by Xiao et al. [33]. The discrete differential form structure can also be preserved using finite elements as shown by He et al. [35] and Kraus et al. [36]. In Ref. [33], the discrete non-canonical Poisson bracket is derived from the discrete Lagrangian, and thus automatically satisfies the Jacobi identity. In Refs. [35] and [36], the discrete bracket is not derived from first-principles, and is confirmed only through involved calculation, where the properties of the finite elements compatible with exterior calculus are crucial.

As discussed above, one of the benefits of symplectic algorithms is the ability to bound for all time-steps the errors of dynamic invariants, such as the energy and momentum. This is well-known and desirable for systems with low dimensions. For the symplectic PIC algorithms, the error on total energy-momentum is bounded. However, the degrees of freedom of a PIC simulation D is large. One or a few constraints imposed by the error bound on the total energy-momentum will not bring a significant improvement over the conventional PIC algorithms. The symplectic condition requires that the algorithm satisfies $D(2D - 1)$ constraints as the exact solution does. Therefore, being symplectic is much stronger than a few constraints on the total energy-momentum. It is stronger than imposing local conservation laws at every space-time grid point, and will result in a significant improvement over the conventional PIC algorithms. However, we note that discrete local energy-momentum conservation is a constraint independent from being symplectic and requires additional geometric structures to be preserved. Xiao et al. [38] showed that the spatially discretized non-canonical VM system of Ref. [30] indeed admits a discrete local energy conservation law. The discrete local momentum conservation law has only been proved from a discrete

Maxwell system by generalizing Noether’s theorem for continuous symmetry groups to discrete symmetry groups [100].

Another important local conservation for PIC algorithms is the conservation of charge, which is first addressed by Eastwood [11], Villasenor and Buneman [13], and Esirkepov [22]. For spatially and temporally discretized systems, Squire et al. [30] pointed out that the discrete local charge conservation is a direct consequence of discrete gauge symmetry. In this paper, we will give a general proof of this fact. Therefore, instead of using special tricks to conserve local charge [11, 13, 22, 101–103], it is much easier to design a Lagrangian discretized in both space and time that is gauge invariant [30, 31, 33–36, 38], and automatically guarantees the local charge conservation.

In this paper, we focus on the structure-preserving geometric PIC algorithms for the VM system, in which the electromagnetic field is discretized in a space-time grid. The algorithms apply to the Vlasov-Poisson system as well. However, for the Vlasov-Poisson system, there exists another approach that is canonically symplectic, pioneered by Cary and Doxas [12]. In this approach, the electrostatic potential is explicitly solved and expressed in terms of particles’ positions, and the Vlasov-Poisson system is transformed into a Hamiltonian system only in terms of particles’ positions and momenta. Since there is no magnetic field, the system is canonically symplectic and can be solved by the standard symplectic integrators for canonical systems [39–53]. This approach is recently adopted by Shadwick et al. [104], Webb [105], and Qiang [106]. Note that this method is effective because the Poisson equation can be solved for the electrostatic potential in terms of particles’ positions by inverting the Laplacian operator. For the VM system, the time-dependent electromagnetic field can not be expressed in terms of particles’ positions and momenta, and the electromagnetic field needs to be treated as an independent dynamic component of the system.

Recently, structure-preserving geometric algorithms have also been developed for the Schrodinger-Maxwell [107] system and the Klein-Gordon-Maxwell system [108, 109], which have important applications in high-energy-density physics. Another noteworthy recent development is the metriplectic particle-in-cell integrators for the Landau collision operator [110].

This paper is organized as follows. In Section II, an introduction to the symplectic integrator is given. Section III presents two simple symplectic PIC examples. Advanced structure-preserving geometric PIC schemes, including a structure-preserving geometric rel-

ativistic PIC algorithm, are given in Section IV. This section also includes a proof of the correspondence between discrete gauge symmetry and discrete charge conservation law, a reformulation of the explicit non-canonical symplectic algorithm for the discrete Poisson bracket using the variational approach, some numerical results and comparison with the conventional Boris-Yee PIC method.

2. SYMPLECTIC INTEGRATORS

The idea of symplectic integrators is to construct discrete one-step iteration maps that preserve the symplectic two-form associated with the original Hamiltonian systems, just as the exact solution maps do. In this section, we briefly describe what this means and how to achieve it. An elementary example is presented to demonstrate the significance of the symplectic method. For more systematic studies and examples, Refs. [39–53] are recommended.

2.1. Hamiltonian systems and the symplectic structure

Hamiltonian system plays an important role in physics. For a canonical Hamiltonian system with N generalized momenta and N generalized coordinates, the dynamics of the system is governed by the canonical Hamiltonian equation

$$\dot{p}_i = -\frac{\partial H}{\partial q_i} , \quad (1)$$

$$\dot{q}_i = \frac{\partial H}{\partial p_i} , \quad (2)$$

where $H = H(p_i, q_i, t)$ is the Hamiltonian function, p_i and q_i are generalized momenta and coordinates. This set of equations can be written in the matrix form,

$$\dot{z} = J^{-1} \nabla H(z) , \quad (3)$$

where

$$J = \begin{bmatrix} 0 & I \\ -I & 0 \end{bmatrix} \quad (4)$$

is the canonical symplectic matrix, I is the $N \times N$ identity matrix, and $z = (p_i, q_i)^T$. The most interesting and useful property of the solution of the canonical Hamiltonian equation

is the preservation of the canonical symplectic structure, i.e., if $z_t(z_0)$ is a solution map of the Hamiltonian system Eq. (3), then the following relation holds,

$$\left(\frac{\partial z_t}{\partial z_0}\right)^T J \left(\frac{\partial z_t}{\partial z_0}\right) = J . \quad (5)$$

Maps with this property are called canonical transformations. A more generalized system is the non-canonical Hamiltonian system (or Poisson system),

$$\dot{z} = \{z, H(z)\} , \quad (6)$$

where z is a vector in an n -dimensional phase space, and $\{\cdot, \cdot\}$ is the Poisson bracket defined as follows. Suppose F , G and H are functions of z , a Poisson bracket is a map which maps two functions F and G into a new function $\{F, G\}$, satisfying the following conditions.

1. Anticommutativity, i.e.,

$$\{F, G\} = -\{G, F\} ; \quad (7)$$

2. Bilinearity, i.e.,

$$\{F + G, H\} = \{F, H\} + \{G, H\} ; \quad (8)$$

3. Product rule, i.e.,

$$\{FG, H\} = \{F, H\} G + F \{G, H\} ; \quad (9)$$

4. Jacobi identity, i.e.,

$$\{F, \{G, H\}\} + \{G, \{H, F\}\} + \{H, \{F, G\}\} = 0 . \quad (10)$$

The Poisson bracket is not only a product operator that satisfies bilinearity and anticommutativity, but also a derivative operator with product rule and Jacobi identity. We can also express the Poisson bracket in the matrix form,

$$\{F, G\} = \left(\frac{\partial F}{\partial z}\right)^T B(z) \frac{\partial G}{\partial z} , \quad (11)$$

where $B(z)$ is an antisymmetric matrix and satisfies

$$\sum_l^n \left(\frac{\partial B_{i,j}(z)}{\partial z_l} B_{l,k}(z) + \frac{\partial B_{j,k}(z)}{\partial z_l} B_{l,i}(z) + \frac{\partial B_{k,i}(z)}{\partial z_l} B_{l,j}(z) \right) = 0 . \quad (12)$$

The equation of motion of the non-canonical Hamiltonian system can be written as

$$\dot{z} = B(z) \frac{\partial H}{\partial z} . \quad (13)$$

The evolution of the non-canonical Hamiltonian system is similar to the canonical case, with the structure matrix $B(z)$ replacing the constant matrix J^{-1} . The solution map of the non-canonical Hamiltonian system $z_t(z_0)$ preserves the non-canonical structure associated with $B(z)$,

$$\frac{\partial z}{\partial z_0} B(z_0) \left(\frac{\partial z}{\partial z_0} \right)^T = B(z) . \quad (14)$$

Here, $\partial z / \partial z_0$ is the Jacobian matrix of $z_t(z_0)$ with respect to z_0 . Note that any non-canonical Hamiltonian system can be locally transformed into a canonical Hamiltonian system according to the Darboux-Lie theorem. However the transformation is in general complicated for practical purpose and does not exist globally.

2.2. Building symplectic algorithms

The first generation of symplectic algorithms by Ruth, Feng, and others [39–42] is constructed by generating functions. For example, for any C^2 function $S_1(P, q)$, the following transformation from (p, q) to (P, Q) ,

$$P = p - \frac{\partial S_1(P, q)}{\partial q} , \quad (15)$$

$$Q = q + \frac{\partial S_1(P, q)}{\partial P} , \quad (16)$$

preserves the canonical symplectic structure. If we choose the generating function as $S_1(P, q) = \Delta t H(P, q)$, then the corresponding transformation

$$\begin{cases} p_{l+1} = p_l - \Delta t H_q(p_{l+1}, q_l) , \\ q_{l+1} = q_l + \Delta t H_p(p_{l+1}, q_l) , \end{cases} \quad (17)$$

is a 1st-order symplectic Euler method, where l is the label of the time step and

$$H_p(p, q) = \frac{\partial H(p, q)}{\partial p} , \quad (18)$$

$$H_q(p, q) = \frac{\partial H(p, q)}{\partial q} . \quad (19)$$

Higher order symplectic schemes can be built using more accurate S_1 . As an example, we can let

$$S_1(P, q) = \Delta t \sum_{i=1}^s b_i H(P_i, Q_i) - h^2 \sum_{i,j=1}^s b_i \hat{a}_{ij} H_q(P_i, Q_i)^T H_p(P_j, Q_j), \quad (20)$$

where

$$P_i = p - h \sum_{j=1}^s \hat{a}_{ij} H_q(P_j, Q_j), \quad (21)$$

$$Q_i = q + h \sum_{j=1}^s a_{ij} H_p(P_j, Q_j), \quad (22)$$

and for all i, j ,

$$b_i \hat{a}_{ij} + b_j a_{ji} = b_i b_j. \quad (23)$$

Then the corresponding symplectic scheme is the symplectic partitioned Runge-Kutta (SPRK) method,

$$P = p - h \sum_{i=1}^s b_i H_q(P_i, Q_i), \quad (24)$$

$$Q = q + h \sum_{i=1}^s b_i H_p(P_i, Q_i). \quad (25)$$

Another method to build symplectic integrators is based on discrete variations developed by Marsden et al. [52, 111, 112], which is a direct generalization of the variational principle. The Lagrangian L of a dynamic system is a function of (q, \dot{q}) , where q is the generalized coordinates $q = (q_1, q_2, \dots, q_m)^T$. The action integral is

$$S[q] = \int_{t_0}^{t_1} L(q, \dot{q}, t) dt. \quad (26)$$

The equation of motion, or the Euler-Lagrange equation, is obtained from

$$\frac{\delta S}{\delta q} \delta q = \lim_{\epsilon \rightarrow 0} \frac{S[q + \epsilon \delta q] - S[q]}{\epsilon} = 0. \quad (27)$$

Here, $\delta q(t)$ is an arbitrary function of t which obeys the boundary condition

$$\delta q(t_0) = \delta q(t_1) = 0. \quad (28)$$

Inserting the S in Eq. (26) into Eq. (27) yields,

$$\frac{\delta S}{\delta q} \delta q = \lim_{\epsilon \rightarrow 0} \frac{1}{\epsilon} \int_{t_0}^{t_1} (L(q + \epsilon \delta q, \dot{q} + \epsilon \delta \dot{q}) - L(q, \dot{q})) dt \quad (29)$$

$$= \int_{t_0}^{t_1} \left(\frac{\partial L(q, \dot{q}, t)}{\partial q} \delta q + \frac{\partial L(q, \dot{q}, t)}{\partial \dot{q}} \delta \dot{q} \right) dt \quad (30)$$

$$= \int_{t_0}^{t_1} \left(\frac{\partial L(q, \dot{q}, t)}{\partial q} - \frac{d}{dt} \frac{\partial L(q, \dot{q}, t)}{\partial \dot{q}} \right) \delta q dt + \frac{\partial L(q, \dot{q}, t)}{\partial \dot{q}} \delta q \Big|_{t_0}^{t_1} = 0 . \quad (31)$$

Using the boundary conditions (28) and the arbitrariness of $\delta q(t)$, we obtain the Euler-Lagrange equation as

$$\frac{\partial L(q, \dot{q}, t)}{\partial q} - \frac{d}{dt} \left(\frac{\partial L(q, \dot{q}, t)}{\partial \dot{q}} \right) = 0 . \quad (32)$$

Now let us build a variational symplectic integrator (VSI) for Eq. (32). Instead of discretizing Eq. (32) directly, the idea of VSI is to discretize the action integral $S[q]$. As an example, let's discuss the following 1st-order VSI. In this method, the action is discretized as

$$S_d = \sum_{l=0}^{N-1} L_d(q_l, q_{l+1}) \Delta t . \quad (33)$$

where

$$L_d(q_l, q_{l+1}) = L \left(q_l, \frac{q_{l+1} - q_l}{\Delta t} \right) , \quad (34)$$

Δt is the time step and N is the total number of time steps. The discrete time advance can be obtained by minimizing the action with respect to q_l ,

$$\frac{\partial S_d}{\partial q_l} = 0, \quad 1 \leq l \leq N-1 . \quad (35)$$

Note that $L_d(q_l, q_{l+1})$ depends only on q_l and q_{l+1} , so Eq. (35) can be simplified as

$$\frac{\partial L_d(q_{l-1}, q_l)}{\partial q_l} + \frac{\partial L_d(q_l, q_{l+1})}{\partial q_l} = 0 . \quad (36)$$

Equation (36) is called the discrete Euler-Lagrange equation [52, 53, 112]. When the values of q_{l-1} and q_l are known, q_{l+1} can be calculated. It is also possible to build high-order variational integrators through high-order discrete action integrals. For example,

$$L_d(l, l+1) = \Delta t \sum_{i=1}^s b_i L(Q_i, \dot{Q}_i) , \quad (37)$$

where

$$Q_i = q_l + \Delta t \sum_{j=1}^s a_{ij} \dot{Q}_j \quad (38)$$

and \dot{Q}_i are chosen to extremize Eq. (37) under the constraints

$$\begin{aligned} \sum_{i=1}^s b_i &= 1 , \\ b_i &\neq 0 , \\ q_{l+1} &= q_l + \Delta t \sum_{i=1}^s b_i \dot{Q}_i . \end{aligned} \tag{39}$$

From this discrete action, we can derive the following variational symplectic partitioned Runge-Kutta (VSPRK) integrator,

$$p_{l+1} = p_l + \Delta t \sum_{i=1}^s b_i \dot{P}_i , \tag{40}$$

$$q_{l+1} = q_l + \Delta t \sum_{i=1}^s b_i \dot{Q}_i , \tag{41}$$

$$P_i = p_l + \Delta t \sum_{j=1}^s \hat{a}_{ij} \dot{P}_j , \tag{42}$$

$$Q_i = q_0 + \Delta t \sum_{j=1}^2 a_{ij} \dot{Q}_j , \tag{43}$$

where

$$\hat{a}_{ij} = b_j - b_j a_{ji} / b_i , \tag{44}$$

$$\dot{P}_i = -H_q (P_i, Q_i) , \tag{45}$$

$$\dot{Q}_i = H_p (P_i, Q_i) , \tag{46}$$

$$H(p, q) = p^T \dot{q}(p, q) - L(q, \dot{q}(p, q)) , \tag{47}$$

$$p = \frac{\partial L}{\partial \dot{q}}(q, \dot{q}) . \tag{48}$$

When the Legendre transformation specified by Eq. (48) is not degenerate, the above VSPRK integrator is equivalent to the previous canonical SPRK integrator given by Eqs. (24) and (25), and the 1st-order variational integrator is equivalent to the 1st-order symplectic Euler method.

For non-canonical Hamiltonian systems, universal symplectic integrator applicable to all non-canonical systems is not known to exist. But it is possible to construct symplectic integrators for specific non-canonical structures. Examples include the symplectic guiding center integrators [63–69] and symplectic integrators for the non-canonical charged particle dynamics in the (\mathbf{x}, \mathbf{v}) coordinate [55–59].

2.3. An example: harmonic oscillator

The simplest Hamiltonian system is the harmonic oscillator, for which the Lagrangian is

$$L(q, \dot{q}) = m \frac{\dot{q}^2}{2} - kq^2 . \quad (49)$$

Here q is the displacement of the oscillator, k and m are positive constants. The equation of motion, or the Euler-Lagrange equation, is

$$\ddot{q} = -\frac{k}{m}q . \quad (50)$$

The system is conservative, and the total energy is an invariant of the dynamics. The orbit is periodic without damping.

Let us build a VSI for it. The Lagrangian can be discretized using the 1st-order forward difference scheme given by Eq. (34). From the discrete Euler-Lagrange equation, we obtain the discrete iteration relation

$$q_{l+1} = 2q_l - q_{l-1} - \Delta t^2 \frac{k}{m} q_l . \quad (51)$$

To test the algorithm, we set $k = m = 1$, $\Delta t = 0.3$, $q_0 = 0$, $\dot{q}_{1/2} = 0.9$, $q_1 = q_0 + \dot{q}_{1/2}\Delta t = 0.027$, and iterate 60000 time steps. For comparison, we also used the standard 4th-order Runge-Kutta method (RK4) to solve the corresponding ODE. The numerical results are shown in Fig. 1. It is clear that even for this simplest Hamiltonian system, the RK4 method failed to preserve the orbit and energy for long-term dynamics. On the other hand for the VSI method, the orbit is well preserved, and the error of energy is bounded by a small value for all simulation time steps.

3. TWO EXAMPLES OF SYMPLECTIC PIC METHODS

In this section we introduce two simple ways to build symplectic PIC integrators, which are based on variational and canonical symplectic methods, respectively. Compared with the algorithms that will be introduced in the next section, these two methods are not charge conservative, and high-order schemes are generally implicit which are not convenient for large scale simulations. But they are good examples to demonstrate the general techniques to build symplectic PIC schemes.

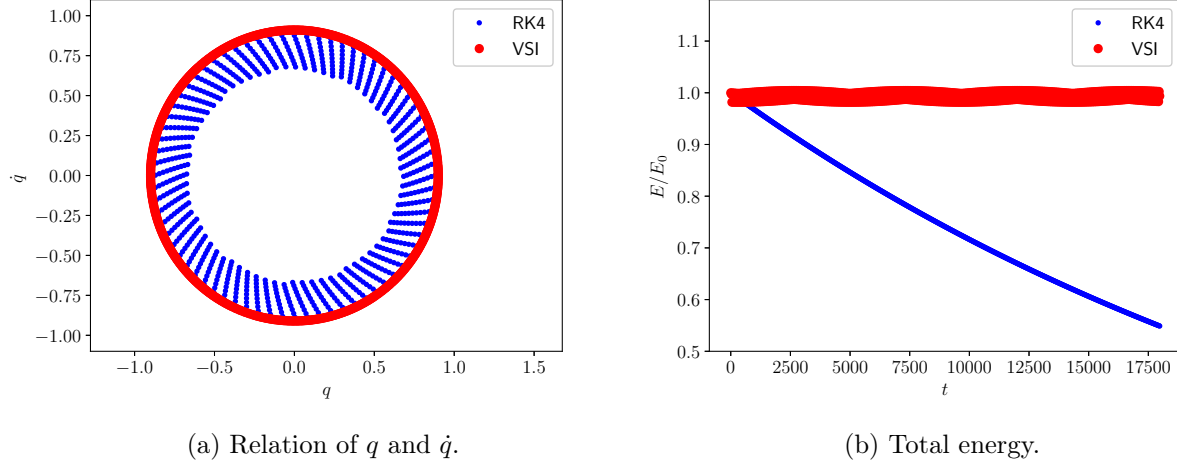


Figure 1: The evolution of the harmonic oscillator in the $q - \dot{q}$ phase space (a), and the evolution of total energy (b) solved by the RK4 and the VSI methods.

According to discussions in the previous section, to construct a symplectic PIC scheme, the starting point is the variational theory for the PIC system. Consider a system that contains a collection of non-relativistic charged particle and electromagnetic fields. The Lagrangian L and action integral S are

$$L = \iiint d\mathbf{x} \left(\frac{\epsilon_0}{2} \left(-\dot{\mathbf{A}}(\mathbf{x}) - \nabla\phi(\mathbf{x}) \right)^2 - \frac{1}{2\mu_0} (\nabla \times \mathbf{A}(\mathbf{x}))^2 + \sum_{s,p} \delta(\mathbf{x} - \mathbf{x}_{sp}) \left(\frac{1}{2} m_s \dot{\mathbf{x}}_{sp}^2 + q_s \mathbf{A}(\mathbf{x}) \cdot \dot{\mathbf{x}}_{sp} - q_s \phi(\mathbf{x}) \right) \right), \quad (52)$$

$$S = \int_0^T L dt, \quad (53)$$

where ϵ_0 and μ_0 are the permittivity and permeability in vacuum, $\mathbf{A}(\mathbf{x})$ and $\phi(\mathbf{x})$ are the vector and scalar potentials of electromagnetic fields, \mathbf{x}_{sp} , m_s and q_s are the location, mass and charge of the p -th particle of species s , respectively. The equations of motion for this particle-field system are determined by the variational principle,

$$\frac{\delta S}{\delta \mathbf{x}_{sp}} = 0, \quad (54)$$

$$\frac{\delta S}{\delta \mathbf{A}} = 0, \quad (55)$$

$$\frac{\delta S}{\delta \phi} = 0. \quad (56)$$

Using the definition of electromagnetic fields $\mathbf{E} = -\dot{\mathbf{A}} - \nabla\phi$ and $\mathbf{B} = \nabla \times \mathbf{A}$, we can easily find that Eqs. (55) and (56) are the Maxwell equations, and Eq. (54) is Newton's equation for particles. Note that the dynamic equation of the particle-field system Eqs. (54)-(56) are gauge symmetric, i.e., they are invariant under the following transform,

$$\mathbf{A} \rightarrow \mathbf{A} + \nabla\psi , \quad (57)$$

$$\phi \rightarrow \phi - \frac{\partial\psi}{\partial t} , \quad (58)$$

where $\psi(\mathbf{x}, t)$ is an arbitrary scalar function.

3.1. Variational symplectic PIC algorithms

Firstly, let us construct a PIC scheme based on the discrete variational principle [31]. This method does not make explicit use of the Hamiltonian structure or any canonical transformation, and all we need is to select a spatial discretization. It is the simplest way to build a symplectic PIC scheme.

From the continuous Lagrangian given by Eq. (52), we observe that particle dynamics does not need any spatial discretization. Fields and interaction between fields and particles can be discretized using grids and interpolating functions. In the simplest case, a cubic mesh can be used, and the fields are discretized on grid points as

$$\mathbf{A}_{i,j,k} \approx \mathbf{A}(i\Delta x, j\Delta x, k\Delta x) , \quad (59)$$

$$\phi_{i,j,k} \approx \phi(i\Delta x, j\Delta x, k\Delta x) , \quad (60)$$

where i, j, k are grid indices in the x, y, z directions and $0 \leq i < N_x, 0 \leq j < N_y, 0 \leq k < N_z$. Here, N_x, N_y, N_z are numbers of grids in the x, y, z directions, respectively, and Δx is the grid size. For discretizing the gradient and curl operators, the forward difference is used. They are defined in Eqs. (A1) and (A2). Since the locations of particles are not always exactly on grid points, to calculate the interaction between particles and electromagnetic fields an interpolating technique is needed. The field interpolated at a given location \mathbf{x} can be written as

$$\mathbf{A}(\mathbf{x}) \approx \sum_{i,j,k} \mathbf{A}_{i,j,k} W(\mathbf{x} - \mathbf{x}_{i,j,k}) , \quad (61)$$

$$\phi(\mathbf{x}) \approx \sum_{i,j,k} \phi_{i,j,k} W(\mathbf{x} - \mathbf{x}_{i,j,k}) , \quad (62)$$

where W is the interpolating function and $\mathbf{x}_{i,j,k}$ is the location of the i, j, k -th grid point, i.e., $\mathbf{x}_{i,j,k} = (i\Delta x, j\Delta x, k\Delta x)$. In general, W should have following properties:

1. It is normalized, i.e., for any \mathbf{x} , $\sum_{i,j,k} W(\mathbf{x}_{i,j,k} + \mathbf{x}) = 1$;
2. It is symmetric, i.e., for any \mathbf{x} , $W(\mathbf{x}) = W(-\mathbf{x})$;
3. It is localized, i.e., when $|\mathbf{x}| > a$, $W(\mathbf{x}) = 0$, where a is the size of the interpolating function;
4. It is smooth for reducing the numerical noise and improving the accuracy.

As an example, the following W given by Ref. [31] is adopted here,

$$\begin{aligned}
 W(\mathbf{x}) &= W_1(x) W_1(y) W_1(z) , \\
 W_1(x) &= \begin{cases} 0 , & x > 2 , \\ \frac{15}{1024}x^8 - \frac{15}{128}x^7 + \frac{49}{128}x^6 - \frac{21}{32}x^5 + \frac{35}{64}x^4 - x + 1 , & 1 < x \leq 2 , \\ -\frac{15}{1024}x^8 - \frac{15}{128}x^7 + \frac{7}{16}x^6 - \frac{21}{32}x^5 + \frac{175}{256}x^4 - \frac{105}{128}x^2 + \frac{337}{512} , & 0 < x \leq 1 , \\ -\frac{15}{1024}x^8 + \frac{15}{128}x^7 + \frac{7}{16}x^6 + \frac{21}{32}x^5 + \frac{175}{256}x^4 - \frac{105}{128}x^2 + \frac{337}{512} , & -1 < x \leq 0 , \\ \frac{15}{1024}x^8 + \frac{15}{128}x^7 + \frac{49}{128}x^6 + \frac{21}{32}x^5 + \frac{35}{64}x^4 + x + 1 , & -2 < x \leq -1 , \\ 0 , & x \leq -2 . \end{cases} \quad (64)
 \end{aligned}$$

This interpolating function is smooth to the third order and piecewise polynomial. It satisfies the above four properties. More discussions on interpolating functions can be found in Refs. [113–116]. To simplify the scheme, we select the temporal gauge $\phi = 0$. In this gauge the electromagnetic fields are

$$\mathbf{E} = -\frac{\partial \mathbf{A}}{\partial t} , \quad (65)$$

$$\mathbf{B} = \nabla \times \mathbf{A} . \quad (66)$$

Using temporal gauge to investigate electrostatic problems may result in numerical overflow due to the continuously increasing vector potential. However in most situations the plasma is quasi-neutral, which means electrostatic field is small, and using temporal gauge

is appropriate. Now the discretized Lagrangian is

$$L_d(\mathbf{x}_{sp}, \dot{\mathbf{x}}_{sp}, \mathbf{A}_{i,j,k}, \dot{\mathbf{A}}_{i,j,k}) = \sum_{i,j,k} \left(\frac{1}{2} \left(-\dot{\mathbf{A}}_{i,j,k} \right)^2 - \frac{1}{2} (\text{curl}_d \mathbf{A}_{i,j,k})^2 \right) + \sum_s \left(\frac{1}{2} m_s \dot{\mathbf{x}}_{sp}^2 + q_s \sum_{i,j,k} \mathbf{A}_{i,j,k} W(\mathbf{x}_{i,j,k} - \mathbf{x}_{sp}) \cdot \dot{\mathbf{x}}_{sp} \right). \quad (67)$$

For the 1st-order variational integrator, the discretized action is

$$S_d = \sum_{l=0}^{N-1} L_d(l, l+1) \Delta t, \quad (68)$$

where

$$L_d(l, l+1) = L_d \left(\mathbf{x}_{sp,l}, \frac{\mathbf{x}_{sp,l+1} - \mathbf{x}_{sp,l}}{\Delta t}, \mathbf{A}_{i,j,k,l}, \frac{\mathbf{A}_{i,j,k,l+1} - \mathbf{A}_{i,j,k,l}}{\Delta t} \right). \quad (69)$$

The final iteration scheme are given by the discrete Euler-Lagrange equations,

$$\frac{\partial S_d}{\partial \mathbf{x}_{sp,l}} = 0, \quad (70)$$

$$\frac{\partial S_d}{\partial \mathbf{A}_{i,j,k,l}} = 0, \quad (71)$$

which are

$$m_s \frac{\mathbf{x}_{sp,l+1} - 2\mathbf{x}_{sp,l} + \mathbf{x}_{sp,l-1}}{\Delta t^2} = q_s \frac{(\mathbf{A}_{l-1}(\mathbf{x}_{sp,l-1}) - \mathbf{A}_l(\mathbf{x}_{sp,l}))}{\Delta t} + \quad (72)$$

$$q_s \nabla \mathbf{A}_l(\mathbf{x}_{sp,l}) \cdot \frac{\mathbf{x}_{sp,l+1} - \mathbf{x}_{sp,l}}{\Delta t}, \quad (73)$$

$$\frac{\mathbf{A}_{i,j,k,l+1} - 2\mathbf{A}_{i,j,k,l} + \mathbf{A}_{i,j,k,l-1}}{\Delta t^2} = -\text{curl}_d^* \text{curl}_d \mathbf{A}_{i,j,k,l} + \mathbf{J}_{i,j,k,l}, \quad (74)$$

where

$$\mathbf{A}_l(\mathbf{x}) = \sum_{i,j,k} \mathbf{A}_{i,j,k,l} W(\mathbf{x} - \mathbf{x}_{i,j,k}), \quad (75)$$

$$\text{curl}_d^* \text{curl}_d \mathbf{A}_{i,j,k,l} = \frac{\partial}{\partial \mathbf{A}_{i,j,k,l}} \sum_{i',j',k'} \frac{1}{2} (\text{curl}_d \mathbf{A})_{i',j',k',l}^2, \quad (76)$$

$$\mathbf{J}_{i,j,k,l} = \sum_{sp} q_s \frac{\mathbf{x}_{sp,l+1} - \mathbf{x}_{sp,l}}{\Delta t} W(\mathbf{x}_{i,j,k} - \mathbf{x}_{sp,l}). \quad (77)$$

Equation (72) is a 3×3 linear equation system for $\mathbf{x}_{sp,l+1}$, and Eq. (74) is an explicit equation of $\mathbf{A}_{i,j,k,l+1}$. The final algorithm is:

1. $\mathbf{A}_{i,j,k,l-1}$, $\mathbf{A}_{i,j,k,l}$, $\mathbf{x}_{sp,l-1}$, $\mathbf{x}_{sp,l}$ are known for the l -th time step;

2. Calculate $\mathbf{x}_{sp,l+1}$ using Eq. (72);
3. Calculate $\mathbf{J}_{i,j,k,l}$ using Eq. (77);
4. Calculate $\mathbf{A}_{i,j,k,l+1}$ using Eq. (74);
5. Set $l = l + 1$ and go to step 1.

Note that $W(\mathbf{x})$ is only locally non-zero near \mathbf{x} , thus the algorithm is locally explicit and convenient to compute in parallel.

3.2. Canonical symplectic PIC algorithm

Another way to build symplectic PIC algorithms is using the canonical symplectic method [34]. The starting point is the discrete Lagrangian for the particle-field system under the temporal gauge. According to the Legendre transformation Eq. (48), the canonical momenta $(\mathbf{p}_{sp}, \mathbf{Y}_{i,j,k})$ are

$$\mathbf{p}_{sp} = \frac{\partial L_d}{\partial \dot{\mathbf{x}}_{sp}} , \quad (78)$$

$$\mathbf{Y}_{i,j,k} = \frac{\partial L_d}{\partial \dot{\mathbf{A}}_{i,j,k}} . \quad (79)$$

The Hamiltonian in terms of the canonical pairs are given by Eq. (47),

$$H_d(\mathbf{x}_{sp}, \mathbf{p}_{sp}, \mathbf{A}_{i,j,k}, \mathbf{Y}_{i,j,k}) = \sum_{sp} \frac{1}{2} \frac{(\mathbf{p}_{sp} - q_s \mathbf{A}(\mathbf{x}_{sp}))^2}{m_s} + \sum_{i,j,k} \frac{1}{2} \left(\frac{\mathbf{Y}_{i,j,k}^2}{\Delta V} + \Delta V (\text{curl}_d \mathbf{A})_{i,j,k}^2 \right) , \quad (80)$$

where

$$\mathbf{A}(\mathbf{x}) = \sum_{i,j,k} \mathbf{A}_{i,j,k} W(\mathbf{x} - \mathbf{x}_{i,j,k}) , \quad (81)$$

Here, the discrete curl_d operator is defined in Eq. (A2). Using the 1st-order symplectic Euler method given by Eq. (17), we obtain the 1st-order canonical symplectic PIC scheme,

$$\frac{\mathbf{x}_{sp,l+1} - \mathbf{x}_{sp,l}}{\Delta t} = \frac{\mathbf{p}_{sp,l+1} - \mathbf{A}_l(\mathbf{x}_{sp,l})}{m_s}, \quad (82)$$

$$\frac{\mathbf{p}_{sp,l+1} - \mathbf{p}_{sp,l}}{\Delta t} = q_s \nabla \mathbf{A}_l(\mathbf{x}_{sp,l}) \cdot (\mathbf{p}_{sp,l+1} - q_s \mathbf{A}_l(\mathbf{x}_{sp,l})), \quad (83)$$

$$\frac{\mathbf{A}_{i,j,k,l+1} - \mathbf{A}_{i,j,k,l}}{\Delta t} = \frac{\mathbf{Y}_{i,j,k,l+1}}{\Delta V}, \quad (84)$$

$$\begin{aligned} \frac{\mathbf{Y}_{i,j,k,l+1} - \mathbf{Y}_{i,j,k,l}}{\Delta t} &= \Delta V (\text{curl}_d^* \text{curl}_d \mathbf{A})_{i,j,k,l} + \\ &\quad \sum_{sp} q_s W(\mathbf{x}_{sp,l} - \mathbf{x}_{i,j,k}) (\mathbf{p}_{sp,l} - q_s \mathbf{A}_{l,l}(\mathbf{x}_{sp,l})). \end{aligned} \quad (85)$$

Here curl_d^* is the transpose of curl_d , as defined in Eq. (A10). We should note that Eq. (83) is a 3×3 linear equation array of $\mathbf{p}_{sp,l+1}$ which is easy to solve, so the whole scheme is also explicit.

It can be proved that this 1st-order canonical symplectic PIC scheme is equivalent to the 1st-order variational symplectic PIC scheme Eqs. (72) and (74) under the following transformation,

$$\frac{\mathbf{x}_{sp,l+1} - \mathbf{x}_{sp,l}}{\Delta t} = \frac{\mathbf{p}_{sp,l+1} - \mathbf{A}_l(\mathbf{x}_{sp,l})}{m_s}, \quad (86)$$

$$\frac{\mathbf{A}_{i,j,k,l+1} - \mathbf{A}_{i,j,k,l}}{\Delta t} = \frac{\mathbf{Y}_{i,j,k,l+1}}{\Delta V}. \quad (87)$$

4. STRUCTURE-PRESERVING GEOMETRIC PIC ALGORITHMS

The variational symplectic and the canonical symplectic PIC schemes discussed above have good long-term conservative properties that conventional PIC schemes do not have. However, they can further improved to preserve more geometric structures and to increase accuracy. In this section, we will describe explicit high-order non-canonical symplectic PIC algorithms that admit a discrete gauge symmetry and a local charge conservation law. To preserve geometric structures such as the symplectic structure and the gauge symmetry, spatial discretization techniques such as discrete exterior calculus (DEC) [117, 118], Whitney interpolating forms [94, 117, 119], and finite element exterior calculus (FEEC) [35, 36] can be used. Here, we will adopt the high-order Whitney interpolating forms developed in Ref. [33]. The algorithm is based on the discrete non-canonical Poisson bracket for the VM system first given in Ref. [33], which automatically satisfies the Jacobi identity since it is derived

from a discrete variational principle. The explicit high-order non-canonical Hamiltonian splitting method for the VM system discovered by He et al. [59, 95] is used. The connection between discrete gauge symmetry and discrete charge conservation law is first pointed out by Squire et al. [30]. We will present a detailed proof of this fact with the help of the Whitney interpolating forms. We will show that the geometric PIC algorithms developed are gauge-symmetric and thus automatically satisfies the charge conservation law. It is also shown that the 1st-order and the 2nd-order geometric PIC algorithms can be equivalently constructed by the discrete variational approach. In addition, a relativistic structure-preserving geometric PIC algorithm is given using the variational approach. Two numerical examples are given to demonstrate the advantages of the structure-preserving geometric PIC algorithms over the conventional PIC schemes.

4.1. Explicit high-order non-canonical symplectic PIC schemes

The starting point of the non-canonical PIC method is also the variational principle of the particle-field system. The Lagrangian density of the system is

$$L = \iiint d\mathbf{x} \left(\frac{\epsilon_0}{2} \left(-\dot{\mathbf{A}}(\mathbf{x}) - \nabla\phi(\mathbf{x}) \right)^2 - \frac{1}{2\mu_0} (\nabla \times \mathbf{A}(\mathbf{x}))^2 + \sum_s \delta(\mathbf{x} - \mathbf{x}_{sp}) \left(\frac{1}{2} m_s \dot{\mathbf{x}}_{sp}^2 + q_s \mathbf{A}(\mathbf{x}) \cdot \dot{\mathbf{x}}_{sp} - q_s \phi(\mathbf{x}) \right) \right). \quad (88)$$

Fields are discretized over a cubic grid mesh, and an interpolating technique is needed to calculate values of fields at the location of particles. It is well-known that electromagnetic field has an intrinsic differential form structure. Thus, we adopt a spatial discretization scheme using the Whitney interpolating forms to preserve this geometric structure. The resulting Lagrangian is

$$L_{sd} = \frac{1}{2} \left(\sum_J \left(-\dot{\mathbf{A}}_J - \sum_I \nabla_{dJ,I} \phi_I \right)^2 - \sum_K \left(\sum_J \text{curl}_{dK,J} \mathbf{A}_J \right)^2 \right) \Delta V + \sum_s \left(\frac{1}{2} m_s \dot{\mathbf{x}}_{sp}^2 + q_s \left(\dot{\mathbf{x}}_{sp} \cdot \sum_J W_{\sigma_1 J}(\mathbf{x}_{sp}) \mathbf{A}_J - \sum_I W_{\sigma_0 I}(\mathbf{x}_{sp}) \phi_I \right) \right), \quad (89)$$

where curl_d and ∇_d are discrete curl and gradient operators, I, J, K, L are the indices for the discrete 0, 1, 2, 3-forms, respectively, $W_{\sigma_0 I}(\mathbf{x})$, $W_{\sigma_1 J}(\mathbf{x})$ and $W_{\sigma_2 K}(\mathbf{x})$ are interpolating functions for discrete 0-forms, 1-forms and 2-forms. To preserve the geometric structure,

interpolating functions and discrete operators are required to satisfy following properties,

$$\nabla \sum_I W_{\sigma_0 I}(\mathbf{x}) \phi_I = \sum_{I,J} W_{\sigma_1 J}(\mathbf{x}) \nabla_{dJ,I} \phi_I , \quad (90)$$

$$\nabla \times \sum_J W_{\sigma_1 J}(\mathbf{x}) \mathbf{A}_J = \sum_{J,K} W_{\sigma_2 K}(\mathbf{x}) \text{curl}_{dK,J} \mathbf{A}_J . \quad (91)$$

These relations are the same as the properties of Whitney interpolating forms [30, 94, 117, 119], in which the interpolating map ϕ_W provides a mechanism to define continuous forms from the discrete ones. For the present application, ϕ_W is either $W_{\sigma_0 I}(\mathbf{x})$ or $W_{\sigma_1 J}(\mathbf{x})$. The map and discrete exterior difference operators satisfy the following rule,

$$\phi_W \mathbf{d} \alpha = \mathbf{d} \phi_W \alpha , \quad (92)$$

where \mathbf{d} and \mathbf{d}_d are the continuous exterior differential and the discrete exterior difference, respectively, and α is an arbitrary discrete form. The original Whitney interpolating map is defined in simplex meshes (e.g., triangle meshes and tetrahedron meshes) and can only affect one grid cell. We have built a new set of interpolating maps which is suitable for cubic meshes and is able to perform high-order interpolation over multiple grid cells [33]. The resulting discrete difference operators and interpolating maps are listed in Eqs. (A1-A7). We should emphasize that for forms with different orders (e.g. vector potential and magnetic field), the resulting interpolating functions are different. Even for different components of the same field in different directions, the interpolating functions are also different. This is very different from conventional interpolating techniques [1–3]. As a result of the structure-preserving properties, the discrete exterior difference operators satisfy

$$\sum_{J,I} \text{curl}_{dK,J} \nabla_{dJ,I} \phi_I = 0 , \quad (93)$$

$$\sum_{K,J} \text{div}_{dL,K} \text{curl}_{dK,J} \mathbf{A}_J = 0 , \quad (94)$$

for any discrete 0-form ϕ_I and 1-form \mathbf{A}_J . These are obviously the discrete analogs of

$$\nabla \times (\nabla \phi) = 0 , \quad (95)$$

$$\nabla \cdot (\nabla \times \mathbf{A}) = 0 . \quad (96)$$

The corresponding equations of motion are

$$\frac{\delta S_{sd}}{\delta \mathbf{A}_J} = 0 , \quad (97)$$

$$\frac{\delta S_{sd}}{\delta \phi_I} = 0 , \quad (98)$$

$$\frac{\delta S_{sd}}{\delta \mathbf{x}_{sp}} = 0 , \quad (99)$$

or more specifically,

$$\ddot{\mathbf{x}}_{sp} = \frac{q_s}{m_s} \left(\dot{\mathbf{x}}_{sp} \times \left(\nabla \times \sum_J \mathbf{A}_J W_{\sigma_1 J}(\mathbf{x}_{sp}) \right) - \sum_J \dot{\mathbf{A}}_J W_{\sigma_1 J}(\mathbf{x}_{sp}) - \sum_I \nabla \phi_I W_{\sigma_0 I}(\mathbf{x}_{sp}) \right) , \quad (100)$$

$$\ddot{\mathbf{A}}_J + \sum_I \nabla_{dJ,I} \dot{\phi}_I = -\text{curl}_d^* \text{curl}_d \mathbf{A}_J + \sum_{sp} q_s \dot{\mathbf{x}}_{sp} W_{\sigma_1 J}(\mathbf{x}_{sp}) , \quad (101)$$

$$0 = \sum_J \nabla_{dJ,I} \left(\dot{\mathbf{A}}_J + \sum_I \nabla_{dJ,I} \phi_I \right) - \sum_{sp} q_s W_{\sigma_0 I}(\mathbf{x}_{sp}) , \quad (102)$$

where S_{sd} is the spatially discretized action integral,

$$S_{sd} = \int dt L_{sd} . \quad (103)$$

Using the property of interpolating maps, we can find that the equations of motion are gauge-free, or symmetric with respect to the electromagnetic gauge, which means that under the following transformation of vector and scalar potentials defined on the grid,

$$\mathbf{A}_J \rightarrow \mathbf{A}_J + \sum_I \nabla_{dJ,I} \psi_I , \quad (104)$$

$$\phi_I \rightarrow \phi_I - \frac{\partial \psi_I}{\partial t} , \quad (105)$$

where ψ_I is an arbitrary discrete 0-form, Eqs. (100-102) do not change.

To obtain an algorithm, we follow Ref. [33] to derive an discrete non-canonical Poisson bracket. Because the dynamical equations are gauge-free, we can choose the temporal gauge $\phi_I = 0$ for simplicity. The corresponding Lagrangian 1-form [120] is

$$\gamma = \frac{\partial L_{sd}}{\partial \dot{q}} d\mathbf{q} - H_{sd} dt \quad (106)$$

where $q = [\mathbf{A}_J, \mathbf{x}_{sp}]$, and H_{sd} is spatially discretized Hamiltonian determined by the Legendre transform,

$$\begin{aligned} H_{sd} &= \frac{\partial L_{sd}}{\partial \dot{q}} \dot{q} - L_{sd} \\ &= \frac{1}{2} \Delta V \left(\sum_J \dot{\mathbf{A}}_J^2 + \sum_K \left(\sum_J \text{curl}_{dK,J} \mathbf{A}_J \right)^2 \right) + \sum_s \frac{1}{2} m_s \dot{\mathbf{x}}_{sp}^2 . \end{aligned} \quad (107)$$

The symplectic 2-form of this system is

$$\Omega = \mathbf{d} \left(\frac{\partial L_{sd}}{\partial \dot{q}} \mathbf{d}q \right) , \quad (108)$$

from which the non-canonical Poisson bracket is

$$\{F, G\} = \left[\frac{\partial F}{\partial \mathbf{A}_J}, \frac{\partial F}{\partial \mathbf{x}_{sp}}, \frac{\partial F}{\partial \dot{\mathbf{A}}_J}, \frac{\partial F}{\partial \dot{\mathbf{x}}_{sp}} \right] \Omega^{-1} \left[\frac{\partial G}{\partial \mathbf{A}_J}, \frac{\partial G}{\partial \mathbf{x}_{sp}}, \frac{\partial G}{\partial \dot{\mathbf{A}}_J}, \frac{\partial G}{\partial \dot{\mathbf{x}}_{sp}} \right]^T , \quad (109)$$

or more specifically

$$\begin{aligned} \{F, G\} &= \frac{1}{\Delta V} \sum_J \left(\frac{\partial F}{\partial \mathbf{A}_J} \cdot \frac{\partial G}{\partial \dot{\mathbf{A}}_J} - \frac{\partial F}{\partial \dot{\mathbf{A}}_J} \cdot \frac{\partial G}{\partial \mathbf{A}_J} \right) + \\ &\quad \sum_s \frac{1}{m_s} \left(\frac{\partial F}{\partial \mathbf{x}_{sp}} \cdot \frac{\partial G}{\partial \dot{\mathbf{x}}_{sp}} - \frac{\partial F}{\partial \dot{\mathbf{x}}_{sp}} \cdot \frac{\partial G}{\partial \mathbf{x}_{sp}} \right) + \\ &\quad \sum_s \frac{q_s}{m_s \Delta V} \left(\frac{\partial G}{\partial \dot{\mathbf{x}}_{sp}} \cdot \sum_J W_{\sigma_{1J}}(\mathbf{x}_{sp}) \frac{\partial F}{\partial \dot{\mathbf{A}}_J} - \frac{\partial F}{\partial \dot{\mathbf{x}}_{sp}} \cdot \sum_J W_{\sigma_{1J}}(\mathbf{x}_{sp}) \frac{\partial G}{\partial \dot{\mathbf{A}}_J} \right) + \\ &\quad - \sum_s \sum_J \frac{q_s}{m_s^2} \frac{\partial F}{\partial \dot{\mathbf{x}}_{sp}} \cdot \left((\nabla \times W_{\sigma_{1J}}(\mathbf{x}_{sp}) \mathbf{A}_J) \times \frac{\partial G}{\partial \dot{\mathbf{x}}_{sp}} \right) . \end{aligned} \quad (110)$$

Now we introduce discrete electromagnetic fields \mathbf{E}_J and \mathbf{B}_K as follows,

$$\mathbf{E}_J = -\dot{\mathbf{A}}_J , \quad (111)$$

$$\mathbf{B}_K = \sum_J \text{curl}_{dK,J} \mathbf{A}_J . \quad (112)$$

Making use of the transformation of partial derivatives with respect to $\mathbf{A}_J, \dot{\mathbf{A}}_J$ and $\mathbf{E}_J, \mathbf{B}_K$,

$$\frac{\partial F}{\partial \mathbf{A}_J} = \sum_K \frac{\partial F}{\partial \mathbf{B}_K} \text{curl}_{dK,J} , \quad (113)$$

$$\frac{\partial F}{\partial \dot{\mathbf{A}}_J} = -\frac{\partial F}{\partial \mathbf{E}_J} , \quad (114)$$

as well as properties of Whitney interpolating maps, we can express the Poisson bracket in terms of $[\mathbf{E}_J, \mathbf{B}_K, \mathbf{x}_{sp}, \dot{\mathbf{x}}_{sp}]$:

$$\begin{aligned} \{F, G\} = & \frac{1}{\Delta V} \sum_J \left(\frac{\partial F}{\partial \mathbf{E}_J} \cdot \sum_K \frac{\partial G}{\partial \mathbf{B}_K} \text{curl}_{\mathbf{d}_{K,J}} - \sum_K \frac{\partial F}{\partial \mathbf{B}_K} \text{curl}_{\mathbf{d}_{K,J}} \cdot \frac{\partial G}{\partial \mathbf{E}_J} \right) + \\ & \sum_s \frac{1}{m_s} \left(\frac{\partial F}{\partial \mathbf{x}_{sp}} \cdot \frac{\partial G}{\partial \dot{\mathbf{x}}_{sp}} - \frac{\partial F}{\partial \dot{\mathbf{x}}_{sp}} \cdot \frac{\partial G}{\partial \mathbf{x}_{sp}} \right) + \\ & \sum_s \frac{q_s}{m_s \Delta V} \left(\frac{\partial F}{\partial \dot{\mathbf{x}}_{sp}} \cdot \sum_J W_{\sigma_{1J}}(\mathbf{x}_{sp}) \frac{\partial G}{\partial \mathbf{E}_J} - \frac{\partial G}{\partial \dot{\mathbf{x}}_{sp}} \cdot \sum_J W_{\sigma_{1J}}(\mathbf{x}_{sp}) \frac{\partial F}{\partial \mathbf{E}_J} \right) + \\ & - \sum_s \frac{q_s}{m_s^2} \frac{\partial F}{\partial \dot{\mathbf{x}}_{sp}} \cdot \left[\sum_K W_{\sigma_{2K}}(\mathbf{x}_{sp}) \mathbf{B}_K \right] \times \frac{\partial G}{\partial \dot{\mathbf{x}}_{sp}} . \end{aligned} \quad (115)$$

And the corresponding Hamiltonian is

$$H_{sd} = \frac{1}{2} \left(\Delta V \sum_J \mathbf{E}_J^2 + \Delta V \sum_K \mathbf{B}_K^2 + \sum_{sp} m_s \dot{\mathbf{x}}_{sp}^2 \right) . \quad (116)$$

The dynamics are then given by the Hamiltonian equations,

$$\dot{F} = \{F, H_{sd}\} , \quad (117)$$

where

$$F = [\mathbf{E}_J, \mathbf{B}_K, \mathbf{x}_{sp}, \dot{\mathbf{x}}_{sp}] . \quad (118)$$

Note that the non-canonical Poisson bracket is defined by the 2-form Ω given by Eq. (108) and thus automatically satisfies the Jacobi identity. This finite dimensional non-canonical Hamiltonian system can be viewed as a Hamiltonian discretization of the continuous VM system [79–81].

Because the Hamiltonian dose not explicitly depend on time t , the total energy is dynamic invariant. Interestingly, there is also a discrete local energy conservation law for this discrete non-canonical Hamiltonian system. Detail discussions of the discrete local energy conservation law can be found in Ref. [38].

Generally speaking, structure-preserving algorithms for non-canonical Hamiltonian systems are difficult to construct. However we found [33] that the high-order explicit Hamiltonian splitting method discovered by He. et al [95] for the continuous VM system is applicable

to our discrete Hamiltonian system. In this method, we split the Hamiltonian into five parts,

$$H_{sd} = H_E + H_B + H_x + H_y + H_z , \quad (119)$$

$$H_E = \frac{1}{2} \Delta V \sum_J \mathbf{E}_J^2 , \quad (120)$$

$$H_B = \frac{1}{2} \Delta V \sum_K \mathbf{B}_K^2 , \quad (121)$$

$$H_r = \frac{1}{2} \sum_{sp} m_s \dot{r}_{sp}^2, \quad \text{for } r \text{ in } x, y, z . \quad (122)$$

It turns out that all of the five Hamiltonian subsystems can be solved analytically, and high-order algorithms for the entire system can be built by compositions.

For H_E and H_B , the corresponding dynamical equations are $\dot{F} = \{F, H_E\}$ and $\dot{F} = \{F, H_B\}$, which are

$$\begin{cases} \dot{\mathbf{E}}_J = 0 , \\ \dot{\mathbf{B}}_K = - \sum_J \text{curl}_{\text{d}K,J} \mathbf{E}_J , \\ \dot{\mathbf{x}}_{sp} = 0 , \\ \ddot{\mathbf{x}}_{sp} = \frac{q_s}{m_s} \sum_J W_{\sigma_{1J}}(\mathbf{x}_{sp}) \mathbf{E}_J . \end{cases} \quad (123)$$

and

$$\begin{cases} \dot{\mathbf{E}}_J = \sum_K \text{curl}_{\text{d}K,J} \mathbf{B}_K , \\ \dot{\mathbf{B}}_K = 0 , \\ \dot{\mathbf{x}}_{sp} = 0 , \\ \ddot{\mathbf{x}}_{sp} = 0 . \end{cases} \quad (124)$$

Their solution maps $\Theta_E(\Delta t)$ and $\Theta_B(\Delta t)$ are

$$\Theta_E(\Delta t) : \begin{cases} \mathbf{E}_J(t + \Delta t) = \mathbf{E}_J(t) , \\ \mathbf{B}_K(t + \Delta t) = \mathbf{B}_K(t) - \Delta t \sum_J \text{curl}_{\text{d}K,J} \mathbf{E}_J(t) , \\ \mathbf{x}_{sp}(t + \Delta t) = \mathbf{x}_{sp}(t) , \\ \dot{\mathbf{x}}_{sp}(t + \Delta t) = \dot{\mathbf{x}}_{sp}(t) + \frac{q_s}{m_s} \Delta t \sum_J W_{\sigma_{1J}}(\mathbf{x}_{sp}(t)) \mathbf{E}_J(t) , \end{cases} \quad (125)$$

and

$$\Theta_B(\Delta t) : \begin{cases} \mathbf{E}_J(t + \Delta t) = \mathbf{E}_J(t) + \Delta t \sum_K \text{curl}_{\text{d}K,J} \mathbf{B}_K(t) , \\ \mathbf{B}_K(t + \Delta t) = \mathbf{B}_K(t) , \\ \mathbf{x}_{sp}(t + \Delta t) = \mathbf{x}_{sp}(t) , \\ \dot{\mathbf{x}}_{sp}(t + \Delta t) = \dot{\mathbf{x}}_{sp}(t) . \end{cases} \quad (126)$$

For H_x , the dynamical equation is $\dot{F} = \{F, H_x\}$, i.e.,

$$\begin{cases} \dot{\mathbf{E}}_J = - \sum_s \frac{q_s}{\Delta V} \dot{x}_{sp} \mathbf{e}_x W_{\sigma_{1J}}(\mathbf{x}_{sp}) , \\ \dot{\mathbf{B}}_K = 0 , \\ \dot{\mathbf{x}}_{sp} = \dot{x}_{sp} \mathbf{e}_x , \\ \ddot{\mathbf{x}}_{sp} = \frac{q_s}{m_s} \dot{x}_{sp} \mathbf{e}_x \times \sum_K W_{\sigma_{2K}}(\mathbf{x}_{sp}) \mathbf{B}_K . \end{cases} \quad (127)$$

And the solution map $\Theta_x(\Delta t)$ is

$$\Theta_x(\Delta t) : \begin{cases} \mathbf{E}_J(t + \Delta t) = \mathbf{E}_J(t) - \int_0^{\Delta t} dt' \sum_s \frac{q_s}{\Delta V} \dot{x}_{sp}(t') \mathbf{e}_x W_{\sigma_{1J}}(\mathbf{x}_{sp}(t') + \dot{x}_{sp}(t') t' \mathbf{e}_x) , \\ \mathbf{B}_K(t + \Delta t) = \mathbf{B}_K(t) , \\ \mathbf{x}_{sp}(t + \Delta t) = \mathbf{x}_{sp}(t) + \Delta t \dot{x}_{sp}(t) \mathbf{e}_x , \\ \dot{\mathbf{x}}_{sp}(t + \Delta t) = \dot{\mathbf{x}}_{sp}(t) + \frac{q_s}{m_s} \dot{x}_{sp}(t) \mathbf{e}_x \times \int_0^{\Delta t} dt' \sum_K W_{\sigma_{2K}}(\mathbf{x}_{sp}(t') + \dot{x}_{sp}(t') t' \mathbf{e}_x) \mathbf{B}_K(t') . \end{cases}$$

Solution maps Θ_y and Θ_z of subsystems with Hamiltonian H_y and H_z respectively can be obtained similarly (see Eqs. (B11, B12)). It is clear that all these solutions are symplectic-structure-preserving, and so are their compositions. Therefore, we can build symplectic schemes for the entire system using compositions. For example, a 1st-order scheme can be chosen as

$$\Theta_1(\Delta t) = \Theta_x(\Delta t) \Theta_y(\Delta t) \Theta_z(\Delta t) \Theta_E(\Delta t) \Theta_B(\Delta t) , \quad (128)$$

a symmetric 2nd-order scheme can be constructed as

$$\begin{aligned} \Theta_2(\Delta t) &= \Theta_E(\Delta t/2) \Theta_x(\Delta t/2) \Theta_y(\Delta t/2) \Theta_z(\Delta t/2) \Theta_B(\Delta t) \\ &\quad \Theta_z(\Delta t/2) \Theta_y(\Delta t/2) \Theta_x(\Delta t/2) \Theta_E(\Delta t/2) , \end{aligned} \quad (129)$$

and a $2(l+1)$ -th order scheme can be constructed from a $2l$ -th order scheme as [121]

$$\Theta_{2(l+1)}(\Delta t) = \Theta_{2l}(\alpha_l \Delta t) \Theta_{2l}(\beta_l \Delta t) \Theta_{2l}(\alpha_l \Delta t) , \quad (130)$$

$$\alpha_l = 1/(2 - 2^{1/(2l+1)}) , \quad (131)$$

$$\beta_l = 1 - 2\alpha_l . \quad (132)$$

Similar or identical structure-preserving geometric PIC algorithms can also be constructed using the discrete variational method. To achieve the charge-conservation property, a gauge-symmetric discrete Lagrangian should be used. The key is to choose a proper integrating

path of charged particles. Squire et al. have found a polyline path to achieve this goal [30]. However, the scheme is implicit. Here, we propose a zigzag path that will render an explicit algorithm. The discrete action is

$$S_d = \sum_{l=0}^{N_t-1} \Delta t L_{\text{dxzig}}(\mathbf{x}_{sp,l}, \mathbf{x}_{sp,l+1}, \mathbf{A}_{J,l}, \mathbf{A}_{J,l+1}, \phi_{I,l}; \Delta t) , \quad (133)$$

$$\begin{aligned} L_{\text{dxzig}}(\mathbf{x}_{sp,l}, \mathbf{x}_{sp,l+1}, \mathbf{A}_{J,l}, \mathbf{A}_{J,l+1}, \phi_{I,l}; \Delta t) = & L_{\text{dfield}} + \\ & \sum_{sp} \left(\frac{1}{2} m_s (\text{Dt}^*(\mathbf{x}_{sp,l+1}))^2 + q_s \left(\text{Dt}^*(\mathbf{x}_{sp,l+1}) \cdot \int_0^1 d\tau \mathbf{A}_l(\mathbf{r}_{\text{zig}}(\mathbf{x}_{sp,l}, \mathbf{x}_{sp,l+1}, \tau)) \right) - \right. \\ & \left. q_s \sum_I W_{\sigma_0 I}(\mathbf{x}_{sp,l}) \phi_{I,l} \right) , \end{aligned} \quad (134)$$

$$L_{\text{dfield}} = \frac{1}{2} \Delta V \left(\sum \left(-\text{Dt}^*(\mathbf{A}_{J,l+1}) - \sum_I \nabla_{\text{d},J,I} \phi_{I,l+1} \right)^2 - \sum_K \left(\sum_J \text{curl}_{\text{d},K,J} \mathbf{A}_{J,l} \right)^2 \right) , \quad (135)$$

where N_t is the number of time steps, and

$$\text{Dt}(f_l) = \frac{f_{l+1} - f_l}{\Delta t} , \quad (136)$$

$$\text{Dt}^*(f_l) = \frac{f_l - f_{l-1}}{\Delta t} , \quad (137)$$

$$\mathbf{A}_l(\mathbf{x}) = \begin{bmatrix} A_{x,l}(\mathbf{x}) , \\ A_{y,l}(\mathbf{x}) , \\ A_{z,l}(\mathbf{x}) \end{bmatrix} = \sum_J W_{\sigma_1 J}(\mathbf{x}) \mathbf{A}_{J,l} , \quad (138)$$

$$\mathbf{r}_{\text{zig}}(\mathbf{x}_1, \mathbf{x}_2, \tau) = \begin{bmatrix} \mathbf{x}_{\text{zig}}(\mathbf{x}_1, \mathbf{x}_2, \tau) , \\ \mathbf{y}_{\text{zig}}(\mathbf{x}_1, \mathbf{x}_2, \tau) , \\ \mathbf{z}_{\text{zig}}(\mathbf{x}_1, \mathbf{x}_2, \tau) \end{bmatrix} = \begin{bmatrix} (x_1 + \tau(x_2 - x_1), y_1, z_1) , \\ (x_2, y_1 + \tau(y_2 - y_1), z_1) , \\ (x_2, y_2, z_1 + \tau(z_2 - z_1)) \end{bmatrix} , \quad (139)$$

$$\mathbf{A}_l(\mathbf{r}_{\text{zig}}(\mathbf{x}_1, \mathbf{x}_2, \tau)) = \begin{bmatrix} A_{x,l}(\mathbf{x}_{\text{zig}}(\mathbf{x}_1, \mathbf{x}_2, \tau)) , \\ A_{y,l}(\mathbf{y}_{\text{zig}}(\mathbf{x}_1, \mathbf{x}_2, \tau)) , \\ A_{z,l}(\mathbf{z}_{\text{zig}}(\mathbf{x}_1, \mathbf{x}_2, \tau)) \end{bmatrix} . \quad (140)$$

Discrete dynamical equations for the fields is obtained from the variation of the discrete action S_d with respect to $\mathbf{A}_{J,l}$, $\phi_{I,l}$, which yields

$$\text{Dt} \left(-\text{Dt}^*(\mathbf{A}_{J,l}) - \sum_I \nabla_{\text{d},J,I} \phi_{I,l} \right) + \text{curl}_{\text{d}}^T \text{curl}_{\text{d}} \mathbf{A}_{J,l} = \mathbf{J}_{J,l} , \quad (141)$$

$$\sum_J \nabla_{\text{d},J,I} \left(-\text{Dt}^*(\mathbf{A}_{J,l}) + \sum_{I'} \nabla_{\text{d},J,I'} \phi_{I',l} \right) = \rho_{I,l} , \quad (142)$$

where

$$\rho_{I,l} = \sum_{sp} q_s W_{\sigma_0 I}(\mathbf{x}_{sp,l}) , \quad (143)$$

$$\mathbf{J}_{J,l} = \sum_{sp} q_s \text{Dt}^*(\mathbf{x}_{sp,l+1}) \cdot \int_0^1 d\tau W_{\sigma_1 J}(\mathbf{r}_{\text{zig}}(\mathbf{x}_{sp,l}, \mathbf{x}_{sp,l+1}, \tau)) . \quad (144)$$

We can also introduce discrete electromagnetic fields as

$$\mathbf{E}_{J,l} = -\text{Dt}^*(\mathbf{A}_{J,l}) - \sum_I \nabla_{\text{d},J,I} \phi_{I,l} , \quad (145)$$

$$\mathbf{B}_{K,l} = \sum_J \text{curl}_{\text{d},K,J} \mathbf{A}_{J,l} . \quad (146)$$

Then Eqs. (141) and (142) become

$$\text{Dt}^*(\mathbf{B}_{K,l}) = - \sum_J \text{curl}_{\text{d},K,J} \mathbf{E}_{J,l} , \quad (147)$$

$$\text{Dt}(\mathbf{E}_{J,l}) = \sum_K \text{curl}_{\text{d}}^*{}_{J,K} \mathbf{B}_{K,l} - \mathbf{J}_{J,l} , \quad (148)$$

$$\sum_J -\nabla_{\text{d},J,I} \mathbf{E}_{J,l} = \rho_{I,l} . \quad (149)$$

In practice, the discrete Poisson equation, i.e., Eq. (149), is automatically satisfied when solving the discrete Maxwell equation, due to the discrete charge conservation property, which will be discussed later. This situation is similar to the continuous case, where the Poisson equation is taken as an initial condition. However, we emphasize that only when the PIC algorithms are able to preserve the discrete charge conservation law, the discrete Poisson equation can be automatically satisfied. Particles' equation of motion is obtained from variation of the discrete S_d with respect to $\mathbf{x}_{sp,l}$. For example, the variation with respect to $x_{sp,l}$ gives the equation to determine $x_{sp,l+1}$,

$$\begin{aligned} m_s \frac{x_{sp,l+1} - 2x_{sp,l} + x_{sp,l-1}}{q_s \Delta t^2} &= \frac{1}{\Delta t} \int_0^1 d\tau A_{x,l-1}(\mathbf{x}_{\text{zig}}(\mathbf{x}_{sp,l-1}, \mathbf{x}_{sp,l}, \tau)) \\ &- \frac{1}{\Delta t} \int_0^1 d\tau A_{x,l}(\mathbf{x}_{\text{zig}}(\mathbf{x}_{sp,l-1}, \mathbf{x}_{sp,l}, \tau)) + \\ &\text{Dt}^*(\mathbf{x}_{sp,l}) \cdot \int_0^1 d\tau \left[\begin{array}{c} \tau \partial_x A_{x,l-1}(\mathbf{x}_{\text{zig}}(\mathbf{x}_{sp,l-1}, \mathbf{x}_{sp,l}, \tau)) , \\ \partial_x A_{y,l-1}(\mathbf{y}_{\text{zig}}(\mathbf{x}_{sp,l-1}, \mathbf{x}_{sp,l}, \tau)) , \\ \partial_x A_{z,l-1}(\mathbf{z}_{\text{zig}}(\mathbf{x}_{sp,l-1}, \mathbf{x}_{sp,l}, \tau)) \end{array} \right] + \\ &\frac{x_{sp,l} - x_{sp,l-1}}{\Delta t} \int_0^1 d\tau (1 - \tau) \partial_x A_{xl}(\mathbf{z}_{\text{zig}}(\mathbf{x}_{sp,l}, \mathbf{x}_{sp,l+1}, \tau)) - \nabla \sum_I W_{\sigma_0 I}(\mathbf{x}_{sp,l}) \phi_{I,l} . \end{aligned} \quad (150)$$

Using following identities,

$$\begin{aligned} & \frac{d}{d\tau} \left(\frac{\tau}{\Delta t} A_{x,l-1} (\mathbf{x}_{\text{zig}} (\mathbf{x}_{sp,l-1}, \mathbf{x}_{sp,l}, \tau)) \right) \\ &= \frac{x_{sp,l} - x_{sp,l-1}}{\Delta t} \tau \partial_x A_{x,l-1} (\mathbf{x}_{\text{zig}} (\mathbf{x}_{sp,l-1}, \mathbf{x}_{sp,l}, \tau)) + \frac{1}{\Delta t} A_{x,l-1} (\mathbf{x}_{\text{zig}} (\mathbf{x}_{sp,l-1}, \mathbf{x}_{sp,l}, \tau)) \quad , \quad (151) \end{aligned}$$

$$\begin{aligned} & \frac{d}{d\tau} \left(\frac{1-\tau}{\Delta t} A_{x,l} (\mathbf{x}_{\text{zig}} (\mathbf{x}_{sp,l}, \mathbf{x}_{sp,l+1}, \tau)) \right) \\ &= \frac{x_{sp,l+1} - x_{sp,l}}{\Delta t} (1-\tau) \partial_x A_{x,l} (\mathbf{x}_{\text{zig}} (\mathbf{x}_{sp,l}, \mathbf{x}_{sp,l+1}, \tau)) - \frac{1}{\Delta t} A_{x,l} (\mathbf{x}_{\text{zig}} (\mathbf{x}_{sp,l}, \mathbf{x}_{sp,l+1}, \tau)) \quad (152) \end{aligned}$$

$$\frac{d}{d\tau} A_{x,l-1} (\mathbf{y}_{\text{zig}} (\mathbf{x}_{sp,l-1}, \mathbf{x}_{sp,l}, \tau)) = \frac{y_{sp,l} - y_{sp,l-1}}{\Delta t} \partial_y A_{x,l-1} (\mathbf{y}_{\text{zig}} (\mathbf{x}_{sp,l-1}, \mathbf{x}_{sp,l}, \tau)) \quad , \quad (153)$$

$$\frac{d}{d\tau} A_{x,l-1} (\mathbf{z}_{\text{zig}} (\mathbf{x}_{sp,l-1}, \mathbf{x}_{sp,l}, \tau)) = \frac{z_{sp,l} - z_{sp,l-1}}{\Delta t} \partial_z A_{x,l-1} (\mathbf{z}_{\text{zig}} (\mathbf{x}_{sp,l-1}, \mathbf{x}_{sp,l}, \tau)) \quad , \quad (154)$$

we can simplify Eq. (150) as

$$\begin{aligned} m_s \frac{x_{sp,l+1} - 2x_{sp,l} + x_{sp,l-1}}{q_s \Delta t^2} &= \left(\frac{\tau}{\Delta t} A_{x,l-1} (\mathbf{x}_{\text{zig}} (\mathbf{x}_{sp,l-1}, \mathbf{x}_{sp,l}, \tau)) \right) \Big|_{\tau=0}^{\tau=1} \\ &+ \left(\frac{1-\tau}{\Delta t} A_{x,l} (\mathbf{x}_{\text{zig}} (\mathbf{x}_{sp,l}, \mathbf{x}_{sp,l+1}, \tau)) \right) \Big|_{\tau=0}^{\tau=1} - \nabla \sum_I W_{\sigma_{0I}} (\mathbf{x}_{sp,l}) \phi_{I,l} + \\ &\text{Dt}^* (\mathbf{x}_{sp,l}) \cdot \int_0^1 d\tau \begin{bmatrix} 0, \\ \partial_x A_{y,l-1} (\mathbf{y}_{\text{zig}} (\mathbf{x}_{sp,l-1}, \mathbf{x}_{sp,l}, \tau)), \\ \partial_x A_{z,l-1} (\mathbf{z}_{\text{zig}} (\mathbf{x}_{sp,l-1}, \mathbf{x}_{sp,l}, \tau)) \end{bmatrix} \\ &= \frac{1}{\Delta t} (A_{x,l-1} (x_{sp,l}, y_{sp,l}, z_{sp,l}) - A_{x,l} (x_{sp,l}, y_{sp,l}, z_{sp,l})) - \nabla \sum_I W_{\sigma_{0I}} (\mathbf{x}_{sp,l}) \phi_{I,l} + \\ &\text{Dt}^* (\mathbf{x}_{sp,l}) \cdot \int_0^1 d\tau \begin{bmatrix} 0, \\ \partial_x A_{y,l-1} (\mathbf{y}_{\text{zig}} (\mathbf{x}_{sp,l-1}, \mathbf{x}_{sp,l}, \tau)) - \partial_y A_{x,l-1} (\mathbf{y}_{\text{zig}} (\mathbf{x}_{sp,l-1}, \mathbf{x}_{sp,l}, \tau)), \\ \partial_x A_{z,l-1} (\mathbf{z}_{\text{zig}} (\mathbf{x}_{sp,l-1}, \mathbf{x}_{sp,l}, \tau)) - \partial_z A_{x,l-1} (\mathbf{z}_{\text{zig}} (\mathbf{x}_{sp,l-1}, \mathbf{x}_{sp,l}, \tau)) \end{bmatrix} \\ &= E_{x,l} (\mathbf{x}_{sp,l}) + \frac{y_{sp,l} - y_{sp,l-1}}{\Delta t} \int_0^1 d\tau B_{z,l-1} (\mathbf{y}_{\text{zig}} (\mathbf{x}_{sp,l-1}, \mathbf{x}_{sp,l}, \tau)) - \\ &\frac{z_{sp,l} - z_{sp,l-1}}{\Delta t} \int_0^1 d\tau B_{y,l-1} (\mathbf{z}_{\text{zig}} (\mathbf{x}_{sp,l-1}, \mathbf{x}_{sp,l}, \tau)) \quad , \quad (155) \end{aligned}$$

where

$$\mathbf{B}_l (\mathbf{x}) = \sum_K W_{\sigma_2 K} (\mathbf{x}) \sum_J \text{curl}_{dK,J} \mathbf{A}_{J,l} = \sum_K W_{\sigma_2 K} (\mathbf{x}) \mathbf{B}_{K,l} \quad , \quad (156)$$

$$\mathbf{E}_l (\mathbf{x}) = \sum_J W_{\sigma_1 J} (\mathbf{x}) \left(\frac{\mathbf{A}_{J,l-1} - \mathbf{A}_{J,l}}{\Delta t} - \sum_I \nabla_{dJ,I} \phi_{I,l} \right) = \sum_J W_{\sigma_1 J} (\mathbf{x}) \mathbf{E}_{J,l} \quad . \quad (157)$$

It clear that Eq. (155) is explicit with respect to $x_{sp,l+1}$. Similar results can be also obtained for solving $y_{sp,l+1}$ and $z_{sp,l+1}$. We thus have a 1st-order symplectic PIC scheme which solves

$\mathbf{x}_{sp,l+1}, \mathbf{E}_{J,l+1}, \mathbf{B}_{K,l+1}$ from $\mathbf{x}_{sp,l}, \mathbf{x}_{sp,l-1}, \mathbf{E}_{J,l}, \mathbf{B}_{K,l}$. If we let $\dot{\mathbf{x}}_{sp,l} = (\mathbf{x}_{sp,l+1} - \mathbf{x}_{sp,l})/\Delta t$, it can be shown that this scheme is equivalent to the 1st-order Hamiltonian splitting scheme Eq. (128). Following this procedure, we can also construct high-order schemes with more accurate discrete Lagrangians. For example, a 2nd-order symmetric symplectic method can be built from the following discrete action,

$$S_{d2} = \sum_{l=0}^{N_t-1} \Delta t L_{\text{dzig2}}(\mathbf{x}_{sp,2l}, \mathbf{x}_{sp,2l+1}, \mathbf{x}_{sp,2l+2}, \mathbf{A}_{J,l}, \mathbf{A}_{J,l+1}, \phi_{I,l}; \Delta t) , \quad (158)$$

$$\begin{aligned} L_{\text{dzig2}}(\mathbf{x}_{sp,2l}, \mathbf{x}_{sp,2l+1}, \mathbf{x}_{sp,2l+2}, \mathbf{A}_{J,l}, \mathbf{A}_{J,l+1}, \phi_{I,l}; \Delta t) = & L_{\text{dfield}} + \\ & \sum_{sp} q_s \left(m_s \left(\frac{\mathbf{x}_{sp,2l+1} - \mathbf{x}_{sp,2l}}{\Delta t} \right)^2 + \frac{\mathbf{x}_{sp,2l+1} - \mathbf{x}_{sp,2l}}{\Delta t} \cdot \int_0^1 d\tau \mathbf{A}_l(\mathbf{r}_{\text{zig}}(\mathbf{x}_{sp,2l}, \mathbf{x}_{sp,2l+1}, \tau)) + \right. \\ & m_s \left(\frac{\mathbf{x}_{sp,2l+2} - \mathbf{x}_{sp,2l+1}}{\Delta t} \right)^2 + \frac{\mathbf{x}_{sp,2l+2} - \mathbf{x}_{sp,2l+1}}{\Delta t} \cdot \int_0^1 d\tau \mathbf{A}_l(\mathbf{r}_{\text{zig}}(\mathbf{x}_{sp,2l+1}, \mathbf{x}_{sp,2l+2}, \tau)) - \\ & \left. \sum_I W_{\sigma_{0I}}(\mathbf{x}_{sp,2l}) \phi_{I,l} \right) . \end{aligned} \quad (159)$$

where the zigzag path \mathbf{r}_{zig} is

$$\mathbf{r}_{\text{zig}}(\mathbf{x}_1, \mathbf{x}_2, \tau) = \begin{bmatrix} (x_1, y_1, z_1 + \tau(z_2 - z_1)) , \\ (x_1, y_1 + \tau(y_2 - y_1), z_2) , \\ (x_1 + \tau(x_2 - x_1), y_2, z_2) \end{bmatrix} . \quad (160)$$

The corresponding equation of motion is again obtained by discrete variation,

$$\frac{\partial S_{d2}}{\partial \mathbf{x}_{sp,l'}} = 0, \quad \text{for } 1 \leq l' \leq 2N_t - 1 , \quad (161)$$

$$\frac{\partial S_{d2}}{\partial \mathbf{A}_{J,l}} = 0, \quad \text{for } 1 \leq l \leq N_t - 1 . \quad (162)$$

It can be proved that this 2nd-order method is the same as the 2nd-order Hamiltonian splitting PIC scheme Eq. (129).

4.2. Structure-preserving geometric relativistic symplectic PIC scheme

In many practical problems, such as runaway electrons in tokamaks, astrophysical plasmas, and high-power laser plasmas, effects of relativistic particles are often significant or dominating. Using the variational formalism, the structure-preserving geometric formalism can be extended to relativistic plasmas.

The Lagrangian for relativistic charged particles and electromagnetic fields is

$$L_r = \iiint d\mathbf{x} \left(\frac{\epsilon_0}{2} \left(-\dot{\mathbf{A}}(\mathbf{x}) - \nabla\phi(\mathbf{x}) \right)^2 - \frac{1}{2\mu_0} (\nabla \times \mathbf{A}(\mathbf{x}))^2 + \sum_{sp} \delta(\mathbf{x} - \mathbf{x}_{sp}) \left(-m_s c^2 \sqrt{1 - (\dot{\mathbf{x}}_{sp}/c)^2} + q_s \mathbf{A}(\mathbf{x}) \cdot \dot{\mathbf{x}}_{sp} - q_s \phi(\mathbf{x}) \right) \right), \quad (163)$$

where m_s is the rest mass of the particle of species s , c is the light speed in the vacuum. The only difference between L_r and the non-relativistic Lagrangian L defined in Eq. (52) is the relativistic mass factor. Most techniques that have been used to discretize the electromagnetic fields and the interaction between particles and electromagnetic fields can be applied to the relativistic case with little modification.

We let $c = \mu_0 = \epsilon_0 = 1$ to simplify the notation. To discretize the relativistic mass factor

$$L_{rp}(\mathbf{x}_{sp}, \dot{\mathbf{x}}_{sp}) = -m_s \sqrt{1 - \dot{\mathbf{x}}_{sp}^2}, \quad (164)$$

we can still use the idea of variational integrator. For example, a 1st-order discretization of this term is

$$L_{rpd1}(\mathbf{x}_{sp,l}, \mathbf{x}_{sp,l+1}; \Delta t) = L_{rp}\left(\mathbf{x}_{sp,l}, \frac{\mathbf{x}_{sp,l+1} - \mathbf{x}_{sp,l}}{\Delta t}\right). \quad (165)$$

And the total Lagrangian and action integral can be discretized by a method similar to that used in deriving Eqs. (134) and (133),

$$S_{rd} = \sum_{l=0}^{N_t-1} \Delta t L_{rd\text{zig}}(\mathbf{x}_{sp,l}, \mathbf{x}_{sp,l+1}, \mathbf{A}_{J,l}, \mathbf{A}_{J,l+1}, \phi_{I,l}; \Delta t), \quad (166)$$

$$L_{rd\text{zig}}(\mathbf{x}_{sp,l}, \mathbf{x}_{sp,l+1}, \mathbf{A}_{J,l}, \mathbf{A}_{J,l+1}, \phi_{I,l}; \Delta t) = L_{d\text{field}} + \sum_{sp} \left(L_{rpd1}(\mathbf{x}_{sp,l}, \mathbf{x}_{sp,l+1}; \Delta t) + q_s \left(\text{Dt}^*(\mathbf{x}_{sp,l+1}) \cdot \int_0^1 d\tau \mathbf{A}_l(\mathbf{r}_{\text{zig}}(\mathbf{x}_{sp,l}, \mathbf{x}_{sp,l+1}, \tau)) \right) - q_s \sum_I W_{\sigma_{0I}}(\mathbf{x}_{sp,l}) \phi_{I,l} \right). \quad (167)$$

The final dynamic equations are derived from the discrete variation,

$$\frac{\partial S_{rd}}{\partial \mathbf{x}_{sp,l}} = 0, \quad (168)$$

$$\frac{\partial S_{rd}}{\partial \mathbf{A}_{J,l}} = 0, \quad (169)$$

$$\frac{\partial S_{rd}}{\partial \phi_{I,l}} = 0. \quad (170)$$

It is found that Eqs. (169) and (170) are the same as Eqs. (141) and (142), respectively. Unfortunately Eq. (168) is no longer explicit, and a nonlinear solver, e.g., the Newton iteration method, is needed to find the solution for every $\mathbf{x}_{sp,l+1}$. But the time advance for the fields is still explicit.

4.3. Discrete gauge symmetry and discrete charge conservation law

For continuous Hamiltonian systems, conservation properties have close connection with Lie group symmetries, as stated by Noether's theorem [122]. For example, the energy-momentum conservation is due to the symmetry of space-time. Such connection for discrete systems have been investigated in the existing literature [38, 52, 53, 111, 123–127]. In this sub-section, we introduce the discrete gauge symmetry and discrete charge conservation law for our geometric PIC schemes. Squire et al. [30] first pointed out the connection between discrete gauge symmetry and discrete charge conservation. Shadwick et al. developed a geometric spatial discretization [104] with gauge invariance for the Vlasov-Poisson system. Charge conservative geometric electromagnetic PIC methods in cubic meshes are developed by Xiao et al. [33], and it has been applied to ideal two-fluid systems as well [97]. FEEC is also used to construct geometric PIC algorithms with discrete gauge symmetry and charged conservation law [35, 36]. The charge conservation property can exist in non-Hamiltonian discrete particle-field systems [11, 13, 22, 101–103, 128, 129].

Now we prove the connection between gauge symmetry and charged conservation law when the system is discretized in both space and time. First, let's define the meaning of discrete gauge symmetry. The discrete system is gauge symmetric, or gauge free, if under the transformation

$$\mathbf{A}_{J,l} \rightarrow \mathbf{A}'_{J,l} = \mathbf{A}_{J,l} + \sum_I \nabla_{dJ,I} \psi_{I,l} , \quad (171)$$

$$\phi_{I,l} \rightarrow \phi'_{I,l} = \phi_{I,l} - \frac{\psi_{I,l} - \psi_{I,l-1}}{\Delta t} , \quad (172)$$

the Lagrangian of the system changes at most by a total time difference term. Here, where $\psi_{I,l}$ is an arbitrary discrete 0-form. Note that this definition of gauge-symmetry is for system that are discrete in both space and time, which is different from the definition (104) and (105) for the systems that are discrete in space but continuous in time.

For discrete Lagrangians of the particle-field system defined by Eqs. (134), (159) and (167), we can prove that they are gauge symmetric. As an example, Let's consider the Lagrangian L_{dxzig} specified by Eq. (134), which contains the following electromagnetic field term L_{dfield} and the interaction term L_{int1} ,

$$L_{\text{dfield}} = \frac{1}{2} \sum_J \left(-\text{Dt}^* (\mathbf{A}_{J,l+1}) - \sum_I \nabla_{\text{d}J,I} \phi_{I,l+1} \right)^2 \Delta V - \frac{1}{2} \sum_K \left(\sum_J \text{curl}_{\text{d}K,J} \mathbf{A}_{J,l} \right)^2 \Delta V, \quad (173)$$

$$L_{\text{int1}} = \sum_{sp} q_s \text{Dt}^* (\mathbf{x}_{sp,l+1}) \cdot \int_0^1 d\tau \mathbf{A}_l (\mathbf{r}_{\text{xzig}} (\mathbf{x}_{sp,l}, \mathbf{x}_{sp,l+1}, \tau)) - \sum_{sp} q_s \sum_I W_{\sigma_0 I} (\mathbf{x}_{sp,l}) \phi_{I,l}. \quad (174)$$

When the discrete field $\mathbf{A}_{J,l}$ and $\phi_{I,l}$ are transformed according to Eqs. (171) and (172), only L_{dfield} and L_{int1} are affected, and total Lagrangian changes into

$$L'_{\text{dxzig}} = L_{\text{dxzig}} + \text{Dt} (F_1(l)), \quad (175)$$

$$F_1(l) = \sum_{sp,I} q_s \psi_{I,l} W_{\sigma_0 I} (\mathbf{x}_{sp,l}). \quad (176)$$

This shows that L_{dxzig} is gauge symmetric. In this case, the discrete action integral only changes by a boundary term,

$$S'_{\text{dzig}} = S_{\text{dzig}} + F_1(N_t) - F_1(0). \quad (177)$$

And discrete dynamic equations do not change under the gauge transform.

In fact, this gauge symmetry implies the charge conservation. The proof is straightforward due to the structure-preserving nature of the space-time discretization. According to Eq. (177), the partial derivative of S'_{dzig} with respect to $\psi_{I,l}$ should be zero when $l \neq 0$ and $l \neq N_t$, which yields

$$\sum_{sp} q_s \left(\text{Dt}^* (\mathbf{x}_{sp,l+1}) \cdot \int_0^1 d\tau \sum_J \nabla_{\text{d}J,I} W_{\sigma_1 J} (\mathbf{r}_{\text{xzig}} (\mathbf{x}_{sp,l}, \mathbf{x}_{sp,l+1}, \tau)) - \text{Dt} (W_{\sigma_0 I} (\mathbf{x}_{sp,l})) \right) = 0. \quad (178)$$

Inserting the $\rho_{I,l}$ and $\mathbf{J}_{J,l}$ defined in Eqs. (143) and (144) into Eq. (178) leads to the discrete charge conservation law,

$$\sum_J \nabla_{\text{d}J,I} \mathbf{J}_{J,l} - \text{Dt} (\rho_{I,l}) = 0, \quad (179)$$

i.e.,

$$\sum_J \text{div}_d^*{}_{I,J} \mathbf{J}_{J,l} + \text{Dt}(\rho_{I,l}) = 0, \quad (180)$$

where div_d^* is the transpose of $-\nabla_d$ defined in Eq. (A11).

If Eq. (149) is satisfied initially, according to Eq. (148),

$$-\sum_J \nabla_{dJ,I} \text{Dt}(\mathbf{E}_{J,l}) = -\sum_J \text{div}_d^*{}_{I,J} \mathbf{J}_{J,l} = \text{Dt}(\rho_{I,l}), \quad (181)$$

we can see that Eq. (149) will be automatically satisfied for all time steps and there is no need to solve it.

Similarly, we can prove that the discrete Lagrangians of the particle-field systems defined by Eqs. (159) and (167) also admit discrete charge conservation law due to the fact that they are gauge symmetric.

4.4. Numeric examples

Using the *C programming language* and the *Message Passing Interface* (MPI), we have implemented the 2nd-order explicit Hamiltonian splitting PIC (EHSPIC) algorithm, the 1st-order variational symplectic charge-conservative relativistic PIC (VSCRPI) algorithm, and the conventional Boris-Yee PIC (BYPIC) scheme for comparison study. Among these PIC schemes, the VSCRPI algorithm is relativistic, and both EHSPIC and VSCRPI algorithms are structure-preserving and geometric. Two numerical examples are given to test and compare these algorithms.

The first example tests the long-term energy conservation property. Simulation parameters are chosen as follows, $n_e = 1.0 \times 10^{19} \text{m}^{-3}$, $q_e = 1.6 \times 10^{-19} \text{C}$, $m_e = 9.1 \times 10^{-31} \text{kg}$, $v_T = 0.02c$, $\mathbf{E}_0 = \mathbf{B}_0 = 0$, $\Delta x = 1.0 \times 10^{-3} \text{m}$, $\Delta t = \Delta x/(2c)$, $N_x = N_y = 16$, and $N_z = 6$. Here, n_e , q_e , m_e and v_T are density, charge, mass and thermal velocity of electrons, which are uniformly distributed in the space and their velocity distribution is Maxwellian. The electromagnetic fields at the initial time are \mathbf{E}_0 and \mathbf{B}_0 , Δx and Δt are the grid size and time step, c is the speed of light in the vacuum, and N_x , N_y and N_z are number of grids at x , y , z directions. Periodic boundary conditions are adopted in all three directions. For each grid cell we put 8 sample particles initially. For these parameters, the plasma frequency is $\omega_{pe} \sim 0.3/\Delta t$. The time history of the total energy obtained in the simulations is plotted

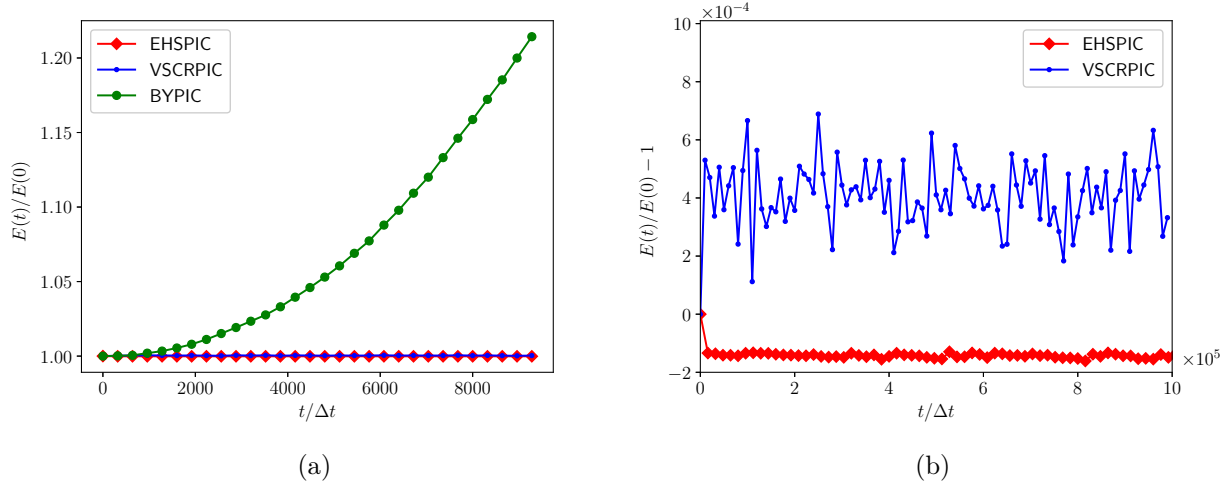


Figure 2: The evolution of total energy calculated by the conventional BYPIC scheme and the structure-preserving VSCRPIK and EHSPIC algorithms in 10^4 time steps (a), and the total energy calculated by two geometric PIC methods in 10^6 time steps.

in Fig. 2. We can clearly see that for BYPIC, the total energy grew significantly after only 10^4 time steps, which is the well-known numerical heating for conventional PIC methods [2, 3, 130]. This numerical difficulty is overcome by the structure-preserving geometric PIC schemes. Even after 10^6 time steps (about $1.67\mu\text{s}$ or $3 \times 10^5/\omega_{pe}$) the error on total energy for EHSPIC and VSCRPIK algorithms is still bounded within a small value.

The second example is the dispersion relation of a hot magnetized plasma. Simulation parameters are chosen as $n_e = 2.5 \times 10^{20}\text{m}^{-3}$, $q_e = 1.6 \times 10^{-19}\text{C}$, $m_e = 9.1 \times 10^{-31}\text{kg}$, $v_T = 0.07c$, $\mathbf{E}_0 = 0$, $\mathbf{B}_0 = B_0\mathbf{e}_x$, $B_0 = 4.6\text{T}$, $\Delta x = 2.0 \times 10^{-5}\text{m}$, $\Delta t = \Delta x/(2c)$, $N_x = N_z = 1$, and $N_y = 256$. Periodic boundaries are used in all 3 directions. Initially we put 200 sample particles in each grid cell. Due to the randomness of particle velocity, electromagnetic perturbation will be excited, and its evolution should satisfy the dispersion relation of a hot magnetized plasma [131]. The space-time spectra of the electric fields in the \mathbf{e}_y direction and time history of the total energy are shown in Fig. 3. These results show that all three methods can recover correctly the analytical dispersion relation. However, the conventional BYPIC method carries a larger low frequency noise in the space-time spectrum (Fig. 3c), which is also reflected by the secular growth of the energy error (Fig. 3d). As expected, the energy error for the two structure-preserving geometric methods is bounded by a small

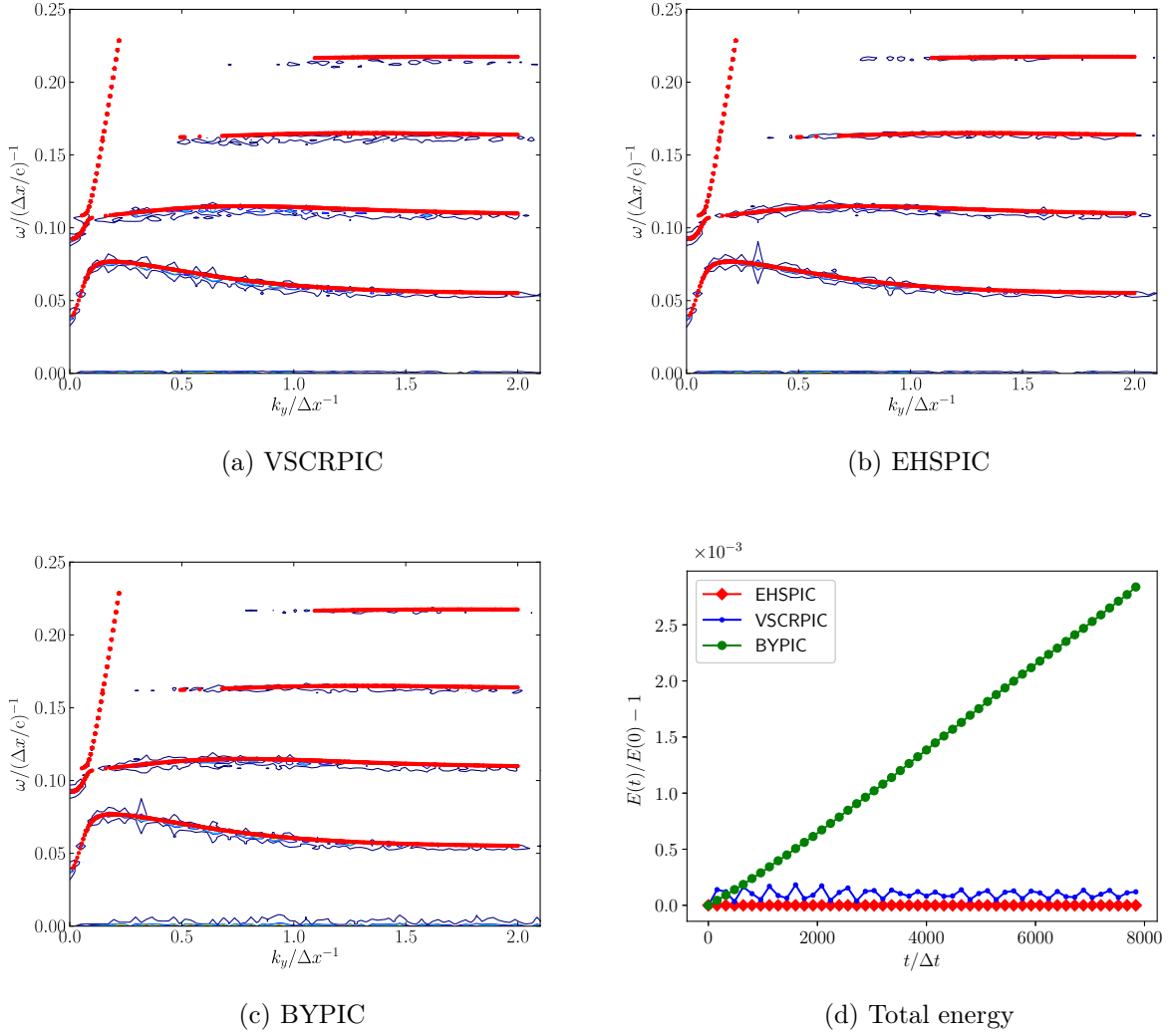


Figure 3: Space-time spectra of electric fields in the \mathbf{e}_y direction of a magnetized hot plasma calculated by the VSCRPIK (a), EHSPIC (b) and BYPIC (c) methods, and time history of energy error for the three PIC schemes (d). Red dots are obtained from the analytical dispersion relation of the corresponding non-relativistic hot magnetized plasma.

number for all simulation time steps. For the VSCRPIK method, the simulated cyclotron frequency of electrons is slightly lower than the non-relativistic analytical value due to the relativistic mass factor.

5. CONCLUSION

PIC algorithms with different types of discretization will lead to very different numerical behaviors. Conventional PIC methods are constructed by discretizing the underpinning integro-differential equations directly, and the schemes in general do not preserve the geometric structures of the Vlasov-Maxwell system. As a consequence, numerical errors accumulate coherently with time and long-term simulation results are not reliable. On the other hand, structure-preserving geometric PIC algorithms developed recently utilize modern mathematical techniques, such as a discrete manifold, interpolating differential forms, and non-canonical symplectic integrators, to ensure gauge symmetry, space-time symmetry and conservation of charge, energy-momentum, and the symplectic structure. These highly desired properties are extremely difficult to achieve using the conventional PIC schemes. The long-term accuracy and fidelity of these geometric algorithms have been demonstrated, and it is our vision that structure-preserving geometric PIC algorithms are most suited for utilizing the upcoming exascale computing power to simulate the complex behavior of laboratory and astrophysical plasmas.

Appendix A: Discrete operators and interpolating forms

For easy reference, we list here all definitions and identities of discrete operators and interpolating forms that are used in this paper. Most of these can be found in Refs. [33, 38, 97].

Let us begin with discrete difference operators,

$$(\nabla_d \phi)_{i,j,k} = [\phi_{i+1,j,k} - \phi_{i,j,k}, \phi_{i,j+1,k} - \phi_{i,j,k}, \phi_{i,j,k+1} - \phi_{i,j,k}] . \quad (\text{A1})$$

$$(\text{curl}_d \mathbf{A})_{i,j,k} = \begin{bmatrix} (A_{zi,j+1,k} - A_{zi,j,k}) - (A_{yi,j,k+1} - A_{yi,j,k}) \\ (A_{xi,j,k+1} - A_{xi,j,k}) - (A_{zi+1,j,k} - A_{zi,j,k}) \\ (A_{yi+1,j,k} - A_{yi,j,k}) - (A_{xi,j+1,k} - A_{xi,j,k}) \end{bmatrix}^T , \quad (\text{A2})$$

$$(\text{div}_d \mathbf{B})_{i,j,k} = (B_{xi+1,j,k} - B_{xi,j,k}) + (B_{yi,j+1,k} - B_{yi,j,k}) + (B_{zi,j,k+1} - B_{zi,j,k}) . \quad (\text{A3})$$

These discrete difference operators are linear, so we also use matrices to denote them. For example, $\nabla_{dJ,I}$ is a $3N \times N$ matrix which maps a discrete scalar field (or 0-form) into a

discrete vector field (or 1-form). Here, $N = N_x \times N_y \times N_z$.

2nd-order Whitney interpolating maps are

$$\sum_{i,j,k} W_{\sigma_0,i,j,k}(\mathbf{x}) \phi_{i,j,k} \equiv \sum_{i,j,k} \phi_{i,j,k} W_1(x) W_1(y) W_1(z), \quad (\text{A4})$$

$$\sum_{i,j,k} W_{\sigma_1,i,j,k}(\mathbf{x}) \mathbf{A}_{i,j,k} \equiv \sum_{i,j,k} \begin{bmatrix} A_{xi,j,k} W_1^{(2)}(x-i) W_1(y-j) W_1(z-k) \\ A_{yi,j,k} W_1(x-i) W_1^{(2)}(y-j) W_1(z-k) \\ A_{zi,j,k} W_1(x-i) W_1(y-j) W_1^{(2)}(z-k) \end{bmatrix}^T, \quad (\text{A5})$$

$$\sum_{i,j,k} W_{\sigma_2,i,j,k}(\mathbf{x}) \mathbf{B}_{i,j,k} \equiv \sum_{i,j,k} \begin{bmatrix} B_{xi,j,k} W_1(x-i) W_1^{(2)}(y-j) W_1^{(2)}(z-k) \\ B_{yi,j,k} W_1^{(2)}(x-i) W_1(y-j) W_1^{(2)}(z-k) \\ B_{zi,j,k} W_1^{(2)}(x-i) W_1^{(2)}(y-j) W_1(z-k) \end{bmatrix}^T, \quad (\text{A6})$$

$$\sum_{i,j,k} W_{\sigma_3,i,j,k}(\mathbf{x}) \rho_{i,j,k} \equiv \sum_{i,j,k} \rho_{i,j,k} W_1^{(2)}(x-i) W_1^{(2)}(y-j) W_1^{(2)}(z-k), \quad (\text{A7})$$

$$W_1^{(2)}(x) = - \begin{cases} W_1'(x) + W_1'(x+1) + W_1'(x+2) & , \quad -1 \leq x < 2, \\ 0 & , \quad \text{otherwise} . \end{cases} \quad (\text{A8})$$

Here, W_1 is a C^2 one-dimensional interpolating function that is only non-zero in the interval $(-2, 2)$, and it can be chosen to be the W_1 defined by Eq. (64).

We have also used the following backward difference operators,

$$(\nabla_d^* \phi)_{i,j,k} = [\phi_{i,j,k} - \phi_{i-1,j,k}, \phi_{i,j,k} - \phi_{i,j-1,k}, \phi_{i,j,k} - \phi_{i,j,k-1}]. \quad (\text{A9})$$

$$(\text{curl}_d^* \mathbf{A})_{i,j,k} = \begin{bmatrix} (A_{zi,j,k} - A_{zi,j-1,k}) - (A_{yi,j,k} - A_{yi,j,k-1}) \\ (A_{xi,j,k} - A_{xi,j,k-1}) - (A_{zi,j,k} - A_{zi-1,j,k}) \\ (A_{yi,j,k} - A_{yi-1,j,k}) - (A_{xi,j,k} - A_{xi,j-1,k}) \end{bmatrix}^T, \quad (\text{A10})$$

$$(\text{div}_d^* \mathbf{B})_{i,j,k} = (B_{xi,j,k} - B_{xi-1,j,k}) + (B_{yi,j,k} - B_{yi,j-1,k}) + (B_{zi,j,k} - B_{zi,j,k-1}). \quad (\text{A11})$$

These operators have close connections with the corresponding forward difference operators,

$$\nabla_{dI,I} = -\text{div}_d^*{}_{I,J}, \quad (\text{A12})$$

$$\text{curl}_{dK,J} = \text{curl}_d^*{}_{J,K}, \quad (\text{A13})$$

$$\text{div}_{dL,K} = -\nabla_{dK,L}^*. \quad (\text{A14})$$

It can be easily checked that these discrete operators and Whitney interpolating maps satisfy following identities,

$$\sum_{J,I} \text{curl}_{dK,J} \nabla_{dJ,I} \phi_I = 0 , \quad (\text{A15})$$

$$\sum_{K,J} \text{div}_{dL,K} \text{curl}_{dK,J} \mathbf{A}_J = 0 , \quad (\text{A16})$$

$$\sum_{K,L} \text{curl}_d^*{}_{J,K} \nabla_{dK,L}^* \phi_L = 0 , \quad (\text{A17})$$

$$\sum_{J,K} \text{div}_d^*{}_{I,J} \text{curl}_d^*{}_{J,K} \mathbf{A}_K = 0 . \quad (\text{A18})$$

$$\nabla \sum_I W_{\sigma_0 I}(\mathbf{x}) \phi_I = \sum_{I,J} W_{\sigma_1 J}(\mathbf{x}) \nabla_{dJ,I} \phi_I , \quad (\text{A19})$$

$$\nabla \times \sum_J W_{\sigma_1 J}(\mathbf{x}) \mathbf{A}_J = \sum_{J,K} W_{\sigma_2 K}(\mathbf{x}) \text{curl}_{dK,J} \mathbf{A}_J . \quad (\text{A20})$$

$$\nabla \times \sum_K W_{\sigma_2 K}(\mathbf{x}) \mathbf{B}_K = \sum_{K,L} W_{\sigma_3 L}(\mathbf{x}) \text{div}_{dL,K} \mathbf{B}_J . \quad (\text{A21})$$

Appendix B: Iteration schemes for PIC methods

In this appendix, we list the three PIC iteration schemes that are used in this work, which are the Boris-Yee PIC (BYPIC) algorithm , the explicit Hamiltonian splitting PIC (EHSPIC) algorithm and the variational symplectic charge-conservative relativistic PIC (VSCRPIK) algorithm.

1. BYPIC scheme

In the BYPIC scheme, electromagnetic fields are solved by using the Yee-FDTD scheme, i.e.,

$$\mathbf{B}_{K,l+1/2} = \mathbf{B}_{K,l-1/2} - \Delta t \sum_J \text{curl}_{dK,J} \mathbf{E}_{K,l} , \quad (\text{B1})$$

$$\mathbf{E}_{J,l+1} = \mathbf{E}_{J,l} + \Delta t \left(\sum_J \text{curl}_d^*{}_{J,K} \mathbf{B}_{K,l+1/2} - \mathbf{J}_{J,l+1/2} \right) . \quad (\text{B2})$$

Positions and velocities of particles are updated by the Boris algorithm, i.e.,

$$\frac{\mathbf{v}_{sp,l+1/2} - \mathbf{v}_{sp,l-1/2}}{\Delta t} = \frac{q_s}{m_s} \left(\mathbf{E}_{sp,l} + \frac{\mathbf{v}_{sp,l+1} + \mathbf{v}_{sp,l}}{2} \times \mathbf{B}_{sp,l} \right) , \quad (\text{B3})$$

$$\frac{\mathbf{x}_{sp,l+1} - \mathbf{x}_{sp,l}}{\Delta t} = \mathbf{v}_{sp,l+1/2} , \quad (\text{B4})$$

where

$$\mathbf{E}_{sp,l} = \sum_J \mathbf{E}_{J,l} W(\mathbf{x}_{sp,l} - \mathbf{x}_J) , \quad (\text{B5})$$

$$\mathbf{B}_{sp,l} = \sum_J \left(\mathbf{B}_{K,l-1/2} - \frac{\Delta t}{2} \sum_J \text{curl}_{dK,J} \mathbf{E}_{K,l} \right) W(\mathbf{x}_{sp,l} - \mathbf{x}_K) , \quad (\text{B6})$$

$$\mathbf{J}_{J,l+1/2} = \sum_{sp} q_s \mathbf{v}_{sp,l+1/2} W\left(\mathbf{x}_{sp,l} + \frac{\Delta t}{2} \mathbf{v}_{sp,l+1/2} - \mathbf{x}_J\right) , \quad (\text{B7})$$

and W is the interpolating function. The initial conditions for the electromagnetic fields and particles' positions and velocities are $\mathbf{B}_{K,-1/2}, \mathbf{E}_{J,0}, \mathbf{x}_{sp,0}, \mathbf{v}_{sp,-1/2}$.

2. EHSPIC scheme

The EHSPIC scheme is a splitting method. As discussed in Sec. 4.4.1, the basic one-step maps for the sub-systems are $\Theta_E(\Delta t), \Theta_B(\Delta t), \Theta_x(\Delta t), \Theta_y(\Delta t), \Theta_z(\Delta t)$, that map $z = [\mathbf{B}_K, \mathbf{E}_J, \mathbf{x}_{sp}, \dot{\mathbf{x}}_{sp}]$ into new $z' = [\mathbf{B}'_K, \mathbf{E}'_J, \mathbf{x}'_{sp}, \dot{\mathbf{x}}'_{sp}]$. They are

$$\Theta_E(\Delta t) : \begin{cases} \mathbf{E}'_J = \mathbf{E}_J , \\ \mathbf{B}'_K = \mathbf{B}_K - \Delta t \sum_J \text{curl}_{dK,J} \mathbf{E}_J , \\ \mathbf{x}'_{sp} = \mathbf{x}_{sp} , \\ \dot{\mathbf{x}}'_{sp} = \dot{\mathbf{x}}_{sp} + \frac{q_s}{m_s} \Delta t \sum_J W_{\sigma_{1J}}(\mathbf{x}_{sp}) \mathbf{E}_J , \end{cases} \quad (\text{B8})$$

$$\Theta_B(\Delta t) : \begin{cases} \mathbf{E}'_J = \mathbf{E}_J + \Delta t \sum_K \text{curl}_{dK,J} \mathbf{B}_K , \\ \mathbf{B}'_K = \mathbf{B}_K , \\ \mathbf{x}'_{sp} = \mathbf{x}_{sp} , \\ \dot{\mathbf{x}}'_{sp} = \dot{\mathbf{x}}_{sp} . \end{cases} \quad (\text{B9})$$

$$\Theta_x(\Delta t) : \begin{cases} \mathbf{E}'_J = \mathbf{E}_J - \int_0^{\Delta t} dt' \sum_s \frac{q_s}{\Delta V} \dot{x}_{sp}(t) \mathbf{e}_x W_{\sigma_{1J}}(\mathbf{x}_{sp} + \dot{x}_{sp} t' \mathbf{e}_x) , \\ \mathbf{B}'_K = \mathbf{B}_K , \\ \mathbf{x}'_{sp} = \mathbf{x}_{sp} + \Delta t \dot{x}_{sp} \mathbf{e}_x , \\ \dot{\mathbf{x}}'_{sp} = \dot{\mathbf{x}}_{sp} + \frac{q_s}{m_s} \dot{x}_{sp} \mathbf{e}_x \times \int_0^{\Delta t} dt' \sum_K W_{\sigma_{2K}}(\mathbf{x}_{sp} + \dot{x}_{sp} t' \mathbf{e}_x) \mathbf{B}_K . \end{cases} \quad (\text{B10})$$

$$\Theta_y(\Delta t) : \begin{cases} \mathbf{E}'_J = \mathbf{E}_J - \int_0^{\Delta t} dt' \sum_s \frac{q_s}{\Delta V} \dot{y}_{sp}(t) \mathbf{e}_y W_{\sigma_{1J}}(\mathbf{x}_{sp} + \dot{y}_{sp} t' \mathbf{e}_y) , \\ \mathbf{B}'_K = \mathbf{B}_K , \\ \mathbf{x}'_{sp} = \mathbf{x}_{sp} + \Delta t \dot{y}_{sp} \mathbf{e}_y , \\ \dot{\mathbf{x}}'_{sp} = \dot{\mathbf{x}}_{sp} + \frac{q_s}{m_s} \dot{y}_{sp} \mathbf{e}_y \times \int_0^{\Delta t} dt' \sum_K W_{\sigma_{2K}}(\mathbf{x}_{sp} + \dot{y}_{sp} t' \mathbf{e}_y) \mathbf{B}_K . \end{cases} \quad (\text{B11})$$

$$\Theta_z(\Delta t) : \begin{cases} \mathbf{E}'_J = \mathbf{E}_J - \int_0^{\Delta t} dt' \sum_s \frac{q_s}{\Delta V} \dot{z}_{sp}(t) \mathbf{e}_z W_{\sigma_{1J}}(\mathbf{x}_{sp} + \dot{z}_{sp} t' \mathbf{e}_z) , \\ \mathbf{B}'_K = \mathbf{B}_K , \\ \mathbf{x}'_{sp} = \mathbf{x}_{sp} + \Delta t \dot{z}_{sp} \mathbf{e}_z , \\ \dot{\mathbf{x}}'_{sp} = \dot{\mathbf{x}}_{sp} + \frac{q_s}{m_s} \dot{z}_{sp} \mathbf{e}_z \times \int_0^{\Delta t} dt' \sum_K W_{\sigma_{2K}}(\mathbf{x}_{sp} + \dot{z}_{sp} t' \mathbf{e}_z) \mathbf{B}_K . \end{cases} \quad (\text{B12})$$

If we use $\Theta_f \Theta_g$ to denote a map that is composed by Θ_f and Θ_g ,

$$(\Theta_f \Theta_g)(z) = \Theta_f(\Theta_g(z)) , \quad (\text{B13})$$

then the 1st-, 2nd- and $2(l+1)$ -th order methods $\Theta_1(\Delta t), \Theta_2(\Delta t), \Theta_{2(l+1)}(\Delta t)$ can be constructed as

$$\Theta_1(\Delta t) = \Theta_x(\Delta t) \Theta_y(\Delta t) \Theta_z(\Delta t) \Theta_E(\Delta t) \Theta_B(\Delta t) , \quad (\text{B14})$$

$$\begin{aligned} \Theta_2(\Delta t) &= \Theta_E(\Delta t/2) \Theta_x(\Delta t/2) \Theta_y(\Delta t/2) \Theta_z(\Delta t/2) \Theta_B(\Delta t) \\ &\quad \Theta_z(\Delta t/2) \Theta_y(\Delta t/2) \Theta_x(\Delta t/2) \Theta_E(\Delta t/2) , \end{aligned} \quad (\text{B15})$$

$$\Theta_{2(l+1)}(\Delta t) = \Theta_{2l}(\alpha_l \Delta t) \Theta_{2l}(\beta_l \Delta t) \Theta_{2l}(\alpha_l \Delta t) , \quad (\text{B16})$$

$$\alpha_l = 1/(2 - 2^{1/(2l+1)}) ,$$

$$\beta_l = 1 - 2\alpha_l .$$

3. VSCRPIE scheme

For the 1st-order VSCRPIE scheme, the algorithm for the electromagnetic fields is,

$$\frac{\mathbf{B}_{K,l} - \mathbf{B}_{K,l-1}}{\Delta t} = - \sum_J \text{curl}_{\text{d}K,J} \mathbf{E}_{J,l} , \quad (\text{B17})$$

$$\frac{\mathbf{E}_{J,l+1} - \mathbf{E}_{J,l}}{\Delta t} = \sum_K \text{curl}_{\text{d}}^*{}_{J,K} \mathbf{B}_{K,l} - \mathbf{J}_{J,l} , \quad (\text{B18})$$

and the algorithm for the dynamics of the sp -th particle is

$$\frac{m_s}{\Delta t} \left(\frac{\mathbf{v}_{sp,l}}{\sqrt{1 - \mathbf{v}_{sp,l}^2}} - \frac{\mathbf{v}_{sp,l-1}}{\sqrt{1 - \mathbf{v}_{sp,l-1}^2}} \right) = q_s \left(\mathbf{E}_{sp,l} + \mathbf{v}_{sp,l-1} \cdot \hat{\mathbf{B}}_{sp,l-1} + \mathbf{v}_{sp,l} \cdot \hat{\mathbf{B}}_{sp,l}^* \right) , \quad (\text{B19})$$

where

$$\mathbf{E}_{sp,l} = \sum_J \mathbf{E}_{J,l} W_{\sigma_1 J}(\mathbf{x}_{sp,l}) , \quad (\text{B20})$$

$$\mathbf{v}_{sp,l-1} \cdot \hat{\mathbf{B}}_{sp,l-1} = \begin{bmatrix} v_{y,sp,l-1} \int_0^1 dt' B_{z,l-1}(x_{sp,l}, y_{sp,l-1} + t'(y_{sp,l} - y_{sp,l-1}), z_{sp,l-1}) - \\ v_{z,sp,l-1} \int_0^1 dt' B_{y,l-1}(x_{sp,l}, y_{sp,l}, z_{sp,l-1} + t'(z_{sp,l} - z_{sp,l-1})) , \\ v_{z,sp,l-1} \int_0^1 dt' B_{x,l-1}(x_{sp,l}, y_{sp,l}, z_{sp,l-1} + t'(z_{sp,l} - z_{sp,l-1})) , \\ 0 \end{bmatrix} , \quad (\text{B21})$$

$$\mathbf{v}_{sp,l} \cdot \hat{\mathbf{B}}_{sp,l}^* = \begin{bmatrix} 0, \\ -v_{x,sp,l} \int_0^1 dt' B_{z,l}(x_{sp,l} + t'(x_{sp,l+1} - x_{sp,l}), y_{sp,l}, z_{sp,l}) , \\ v_{x,sp,l} \int_0^1 dt' B_{y,l}(x_{sp,l} + t'(x_{sp,l+1} - x_{sp,l}), y_{sp,l}, z_{sp,l}) - \\ v_{y,sp,l} \int_0^1 dt' B_{x,l}(x_{sp,l+1}, y_{sp,l} + t'(y_{sp,l+1} - y_{sp,l}), z_{sp,l}) \end{bmatrix} , \quad (\text{B22})$$

$$\mathbf{v}_{sp,l} = \frac{\mathbf{x}_{sp,l+1} - \mathbf{x}_{sp,l}}{\Delta t} , \quad (\text{B23})$$

$$\begin{bmatrix} B_{x,l}(\mathbf{x}) , \\ B_{y,l}(\mathbf{x}) , \\ B_{z,l}(\mathbf{x}) \end{bmatrix} = \sum_K \mathbf{B}_{K,l} W_{\sigma_2 K}(\mathbf{x}) , \quad (\text{B24})$$

$$\mathbf{J}_{J,l} = \sum_{sp} q_s \text{Dt}^*(\mathbf{x}_{sp,l+1}) \cdot \int_0^1 d\tau W_{\sigma_1 J}(\mathbf{r}_{\text{xxig}}(\mathbf{x}_{sp,l}, \mathbf{x}_{sp,l+1}, \tau)) . \quad (\text{B25})$$

ACKNOWLEDGMENTS

This research is supported by National Natural Science Foundation of China (NSFC-11775219, 11775222, 11505186, 11575185 and 11575186), National Key Research and Development Program (2016YFA0400600, 2016YFA0400601 and 2016YFA0400602), ITER-China Program (2015GB111003, 2014GB124005) Chinese Scholar Council (201506340103), China Postdoctoral Science Foundation (2017LH002), and the GeoAlgorithmic Plasma Simulator (GAPS) Project.

- [2] R. W. Hockney and J. W. Eastwood, *Computer Simulation Using Particles* (CRC Press, 1988).
- [3] C. K. Birdsall and A. B. Langdon, *Plasma Physics via Computer Simulation* (IOP Publishing, 1991) p. 293.
- [4] H. Okuda, *Journal of Computational Physics* **10**, 475 (1972).
- [5] B. I. Cohen, A. B. Langdon, and A. Friedman, *Journal of Computational Physics* **46**, 15 (1982).
- [6] A. B. Langdon, B. I. Cohen, and A. Friedman, *Journal of Computational Physics* **51**, 107 (1983).
- [7] W. W. Lee, *Physics of Fluids* **26**, 556 (1983).
- [8] B. I. Cohen, A. B. Langdon, D. W. Hewett, and R. J. Procassini, *Journal of Computational Physics* **81**, 151 (1989).
- [9] P. C. Liewer and V. K. Decyk, *Journal of Computational Physics* **85**, 302 (1989).
- [10] A. Friedman, S. E. Parker, S. L. Ray, and C. K. Birdsall, *Journal of Computational Physics* **96**, 54 (1991).
- [11] J. W. Eastwood, *Computer Physics Communications* **64**, 252 (1991).
- [12] J. Cary and I. Dexas, *Journal of Computational Physics* **107**, 98 (1993).
- [13] J. Villasenor and O. Buneman, *Computer Physics Communications* **69**, 306 (1992).
- [14] S. E. Parker, W. W. Lee, and R. A. Santoro, *Physical Review Letters* **71**, 2042 (1993).
- [15] D. P. Grote, A. Friedman, I. Haber, W. Fawley, and J. L. Vay, *Nuclear Instruments and Methods in Physics Research A* **415**, 428 (1998).
- [16] V. K. Decyk, *Computer Physics Communications* **87**, 87 (1995).
- [17] H. Qin, R. C. Davidson, and W. W. Lee, *Physical Review Special Topics - Accelerators and Beams* **3**, 084401 (2000).
- [18] H. Qin, R. C. Davidson, and W. W. Lee, *Physics Letters A* **272**, 389 (2000).
- [19] J. Qiang, R. D. Ryne, S. Habib, and V. Decyk, *Journal of Computational Physics* **163**, 434 (2000).
- [20] Y. Chen and S. E. Parker, *Journal of Computational Physics* **189**, 463 (2003).
- [21] H. Qin, R. C. Davidson, W. W. Lee, and R. Kolesnikov, *Nuclear Instruments and Methods in Physics Research Section A* **464**, 477 (2001).
- [22] T. Z. Esirkepov, *Computer Physics Communications* **135**, 144 (2001).

- [23] J.-L. Vay, P. Colella, P. McCorquodale, B. van Straalen, A. Friedman, and D. P. Grote, *Laser and Particle Beams* **20**, 569 (2002).
- [24] C. Nieter and J. R. Cary, *Journal of Computational Physics* **196**, 448 (2004).
- [25] C. Huang, V. K. Decyk, C. Ren, M. Zhou, W. Lu, W. B. Mori, J. H. Cooley, T. M. Antonsen, and T. Katsouleas, *Journal of Computational Physics* **217**, 658 (2006).
- [26] G. Chen, L. Chacón, and D. C. Barnes, *Journal of Computational Physics* **230**, 7018 (2011).
- [27] R. C. Davidson and H. Qin, “Physics of intense charged particle beams in high energy accelerators,” (Imperial College Press and World Scientific, 2001).
- [28] H. Fu, J. Liao, J. Yang, L. Wang, Z. Song, X. Huang, C. Yang, W. Xue, F. Liu, F. Qiao, *et al.*, *Science China Information Sciences* **59**, 072001 (2016).
- [29] J. Liu, H. Qin, Y. Wang, G. Yang, J. Zheng, Y. Yao, Y. Zheng, Z. Liu, and X. Liu, *arXiv:1611.02362* (2016).
- [30] J. Squire, H. Qin, and W. M. Tang, *Physics of Plasmas* **19**, 084501 (2012).
- [31] J. Xiao, J. Liu, H. Qin, and Z. Yu, *Physics of Plasmas* **20**, 102517 (2013).
- [32] J. Xiao, J. Liu, H. Qin, Z. Yu, and N. Xiang, *Physics of Plasmas* **22**, 092305 (2015).
- [33] J. Xiao, H. Qin, J. Liu, Y. He, R. Zhang, and Y. Sun, *Physics of Plasmas* **22**, 112504 (2015).
- [34] H. Qin, J. Liu, J. Xiao, R. Zhang, Y. He, Y. Wang, Y. Sun, J. W. Burby, L. Ellison, and Y. Zhou, *Nuclear Fusion* **56**, 014001 (2016).
- [35] Y. He, Y. Sun, H. Qin, and J. Liu, *Physics of Plasmas* **23**, 092108 (2016).
- [36] M. Kraus, K. Kormann, P. J. Morrison, and E. Sonnendrücker, *Journal of Plasma Physics* **83** (2017).
- [37] P. J. Morrison, *Physics of Plasmas* **24**, 055502 (2017).
- [38] J. Xiao, H. Qin, J. Liu, and R. Zhang, *Physics of Plasmas* **24**, 062112 (2017).
- [39] R. D. Ruth, *IEEE Transcript on Nuclear Science* **30**, 2669 (1983).
- [40] K. Feng, in *the Proceedings of 1984 Beijing Symposium on Differential Geometry and Differential Equations*, edited by K. Feng (Science Press, 1985) pp. 42–58.
- [41] K. Feng, *Journal of Computational Mathematics* **4**, 279 (1986).
- [42] K. Feng and M. Qin, *Symplectic Geometric Algorithms for Hamiltonian Systems* (Springer, 2010).
- [43] E. Forest and R. D. Ruth, *Physica D* **43**, 105 (1990).
- [44] P. J. Channell and C. Scovel, *Nonlinearity* **3**, 231 (1990).

- [45] J. Candy and W. Rozmus, *Journal of Computational Physics* **92**, 230 (1991).
- [46] J. Hong and M. Qin, *Applied Mathematics Letters* **15**, 1005 (2002).
- [47] Y. Tang, *Computers & Mathematics with Applications* **25**, 83 (1993).
- [48] Z. Shang, *Journal of Computational Mathematics* **2**, 265 (1994).
- [49] Z. Shang, *Numerische Mathematik* **83**, 477 (1999).
- [50] J. M. Sanz-Serna and M. P. Calvo, *Numerical Hamiltonian Problems* (Chapman and Hall, London, 1994).
- [51] Y. Sun and M. Qin, *Journal of Mathematical Physics* **41**, 7854 (2000).
- [52] J. E. Marsden and M. West, *Acta Numerica* **10**, 357 (2001).
- [53] E. Hairer, C. Lubich, and G. Wanner, *Geometric Numerical Integration: Structure-preserving Algorithms for Ordinary Differential Equations*, Vol. 31 (Springer, 2006).
- [54] R. Devogelaere, *Methods of Integration Which Preserve the Contact Transformation Property of the Hamilton Equations*, Tech. Rep. (University of Notre Dame, 1956).
- [55] R. Zhang, H. Qin, Y. Tang, J. Liu, Y. He, and J. Xiao, *Physical Review E* **94**, 013205 (2016).
- [56] Y. Wang, J. Liu, and H. Qin, *Physics of Plasmas* **23**, 122513 (2016).
- [57] Z. Zhou, Y. He, Y. Sun, J. Liu, and H. Qin, *Physics of Plasmas* **24**, 052507 (2017).
- [58] R. Zhang, Y. Wang, Y. He, J. Xiao, J. Liu, H. Qin, and Y. Tang, *Physics of Plasmas* **25**, 022117 (2018), 1610.05390v1.
- [59] Y. He, Z. Zhou, Y. Sun, J. Liu, and H. Qin, *Physics Letters A* **381**, 568 (2017).
- [60] R. G. Littlejohn, *Journal of Mathematical Physics* **20**, 2445 (1979).
- [61] R. G. Littlejohn, *Physics of Fluids* **24**, 1730 (1981).
- [62] R. G. Littlejohn, *J. Plasma Phys* **29**, 111 (1983).
- [63] H. Qin and X. Guan, *Physical Review Letters* **100**, 035006 (2008).
- [64] H. Qin, X. Guan, and W. M. Tang, *Physics of Plasmas* **16**, 042510 (2009).
- [65] R. Zhang, J. Liu, Y. Tang, H. Qin, J. Xiao, and B. Zhu, *Physics of Plasmas* **21**, 032504 (2014).
- [66] C. L. Ellison, J. M. Finn, H. Qin, and W. M. Tang, *Plasma Physics and Controlled Fusion* **57**, 054007 (2015).
- [67] J. Burby and C. Ellison, *Physics of Plasmas* **24**, 110703 (2017).
- [68] M. Kraus, *arXiv:1708.07356* (2017).

- [69] C. L. Ellison, J. M. Finn, J. W. Burby, M. Kraus, H. Qin, and W. M. Tang, arXiv:1801.07240 (2018).
- [70] H. Qin, S. Zhang, J. Xiao, J. Liu, Y. Sun, and W. M. Tang, *Physics of Plasmas* **20**, 084503 (2013).
- [71] R. Zhang, J. Liu, H. Qin, Y. Wang, Y. He, and Y. Sun, *Physics of Plasmas* **22**, 044501 (2015).
- [72] Y. He, Y. Sun, J. Liu, and H. Qin, *Journal of Computational Physics* **281**, 135 (2015).
- [73] Y. He, Y. Sun, R. Zhang, Y. Wang, J. Liu, and H. Qin, *Physics of Plasmas* **23**, 092109 (2016).
- [74] Y. He, Y. Sun, J. Liu, and H. Qin, *Journal of Computational Physics* **305**, 172 (2016).
- [75] X. Tu, B. Zhu, Y. Tang, H. Qin, J. Liu, and R. Zhang, *Physics of Plasmas* **23**, 122514 (2016).
- [76] A. V. Higuera and J. R. Cary, *Physics of Plasmas* **24**, 052104 (2017).
- [77] J. Boris, in *Proceedings of the Fourth Conference on Numerical Simulation of Plasmas* (Naval Research Laboratory, Washington D. C., 1970) p. 3.
- [78] C. Ellison, J. Burby, and H. Qin, *Journal of Computational Physics* **301**, 489 (2015).
- [79] P. J. Morrison, *Physics Letters A* **80**, 383 (1980).
- [80] J. E. Marsden and A. Weinstein, *Physica D: Nonlinear Phenomena* **4**, 394 (1982).
- [81] P. J. Morrison, *Reviews of Modern Physics* **70**, 467 (1998).
- [82] J. Squire, H. Qin, W. Tang, and C. Chandre, *Physics of Plasmas* **20**, 022501 (2013).
- [83] H. Qin, J. W. Burby, and R. C. Davidson, *Physical Review E* **90**, 043102 (2014).
- [84] R. G. Spencer and A. N. Kaufman, *Physical Review A* **25**, 2437 (1982).
- [85] P. J. Morrison and J. M. Greene, *Physical Review Letters* **45**, 790 (1980).
- [86] H. Qin, *Fields Institute Communications* **46**, 171 (2005).
- [87] H. Qin, R. Cohen, W. Nevins, and X. Xu, *Physics of Plasmas* **14**, 056110 (2007).
- [88] J. Burby, A. Brizard, P. Morrison, and H. Qin, *Physics Letters A* **379**, 2073 (2015).
- [89] F. E. Low, *Proceedings of the Royal Society of London Series A* **248**, 282 (1958).
- [90] H. R. Lewis, *Journal of Computational Physics* **6**, 136 (1970).
- [91] H. R. Lewis, *Journal of Computational Physics* **10**, 400 (1972).
- [92] E. Evstatiev and B. Shadwick, *Journal of Computational Physics* **245**, 376 (2013).
- [93] A. B. Stamm, B. A. Shadwick, and E. G. Evstatiev, *IEEE Transactions on Plasma Science* **42**, 1747 (2014).

- [94] H. Whitney, *Geometric Integration Theory* (Princeton University Press, 1957).
- [95] Y. He, H. Qin, Y. Sun, J. Xiao, R. Zhang, and J. Liu, *Physics of Plasmas* **22**, 124503 (2015).
- [96] J. W. Burby, *Physics of Plasmas* **24**, 032101 (2017).
- [97] J. Xiao, H. Qin, P. J. Morrison, J. Liu, Z. Yu, R. Zhang, and Y. He, *Physics of Plasmas* **23**, 112107 (2016).
- [98] N. Crouseilles, L. Einkemmer, and E. Faou, *Journal of Computational Physics* **283**, 224 (2015).
- [99] H. Qin, Y. He, R. Zhang, J. Liu, J. Xiao, and Y. Wang, *Journal of Computational Physics* **297**, 721 (2015).
- [100] J. Xiao, H. Qin, Y. Shi, J. Liu, and R. Zhang, arXiv:1709.09593 (2017).
- [101] T. Umeda, Y. Omura, T. Tominaga, and H. Matsumoto, *Computer Physics Communications* **156**, 73 (2003).
- [102] M. C. Pinto, S. Jund, S. Salmon, and E. Sonnendrücker, *Comptes Rendus Mecanique* **342**, 570 (2014).
- [103] H. Moon, F. L. Teixeira, and Y. A. Omelchenko, *Computer Physics Communications* **194**, 43 (2015).
- [104] B. A. Shadwick, A. B. Stamm, and E. G. Evstatiev, *Physics of Plasmas* **21**, 055708 (2014).
- [105] S. D. Webb, *Plasma Physics and Controlled Fusion* **58**, 034007 (2016).
- [106] J. Qiang, arXiv:1610.04763 (2016).
- [107] Q. Chen, H. Qin, J. Liu, J. Xiao, R. Zhang, Y. He, and Y. Wang, *Journal of Computational Physics* **349**, 441 (2017).
- [108] Y. Shi, N. J. Fisch, and H. Qin, *Physical Review A* **94**, 012124 (2016).
- [109] Y. Shi, J. Xiao, H. Qin, and N. J. Fisch, arXiv:1802.00524v1 (2018).
- [110] E. Hirvijoki, M. Kraus, and J. W. Burby, arXiv:1802.05263 (2018).
- [111] J. M. Wendlandt and J. E. Marsden, *Physica D: Nonlinear Phenomena* **106**, 223 (1997).
- [112] J. E. Marsden, G. W. Patrick, and S. Shkoller, *Communications in Mathematical Physics* **199**, 351 (1998).
- [113] L. B. Lucy, *The Astronomical Journal* **82**, 1013 (1977).
- [114] J. J. Monaghan, *Annual Review of Astronomy and Astrophysics* **30**, 543 (1992).
- [115] G. Liu and M. B. Liu, *Smoothed particle hydrodynamics: a meshfree particle method* (World Scientific, 2003).

- [116] D. J. Price and J. Monaghan, Monthly Notices of the Royal Astronomical Society **348**, 139 (2004).
- [117] A. N. Hirani, *Discrete Exterior Calculus*, Ph.D. thesis, California Institute of Technology (2003).
- [118] A. Stern, Y. Tong, M. Desbrun, and J. E. Marsden, in *Geometry, Mechanics, and Dynamics* (Springer, 2015) pp. 437–475.
- [119] M. Desbrun, E. Kanso, and Y. Tong, in *Discrete Differential Geometry* (Springer, 2008) pp. 287–324.
- [120] J. E. Marsden and T. Ratiu, *Introduction to mechanics and symmetry: a basic exposition of classical mechanical systems*, Vol. 17 (Springer Science & Business Media, 2013).
- [121] H. Yoshida, Physics Letters A **150**, 262 (1990).
- [122] E. Noether, Transport Theory and Statistical Physics **1**, 186 (1971).
- [123] T. Lee, Journal of Statistical Physics **46**, 843 (1987).
- [124] V. Dorodnitsyn, Applied Numerical Mathematics **39**, 307 (2001).
- [125] P. E. Hydon and E. L. Mansfield, Proceedings of the Royal Society of London A: Mathematical, Physical and
- [126] V. Dorodnitsyn, *Applications of Lie Groups to Difference Equations* (CRC Press, Boca Raton, 2011).
- [127] P. E. Hydon, *Difference Equations by Differential Equation Methods* (Cambridge Univ Press, 2014) p. 183.
- [128] O. Buneman and W. Pardo, *Relativistic Plasmas* (Benjamin, New York, 1968) p. 205.
- [129] R. Morse and C. Nielson, The Physics of Fluids **14**, 830 (1971).
- [130] H. Ueda, Y. Omura, H. Matsumoto, and T. Okuzawa, Computer Physics Communications **79**, 249 (1994).
- [131] T. H. Stix, *Waves in Plasmas* (Springer, 1992) pp. 276–277.